arXiv:cond-mat/9903416v3 [cond-mat.mes-hall] 6 Apr 1999

Effects of Domain Wall on Electronic Transport Properties in Mesoscopic Wire of Metallic Ferromagnets

Gen Tatara
Max Planck Institut fur Mikrostrukturphysik, Weinberg 2, D-06120 Halle, Germany
and
Graduate School of Science, Osaka University, Toyonaka, Osaka 560-0043

We study the effect of the domain wall on electronic transport properties in wire of ferromagnetic $3d$ transition metals based on the linear response theory. We considered the exchange interaction between the conduction electron and the magnetization, taking into account the scattering by impurities as well. The effective electron-wall interaction is derived by use of a local gauge transformation in the spin space. This interaction is treated perturbatively to the second order. The conductivity contribution within the classical (Boltzmann) transport theory turns out to be negligiblly small in bulk magnets, due to a large thickness of the wall compared with the fermi wavelength. It can be, however, significant in ballistic nanocontacts, as indicated in recent experiments. We also discuss the quantum correction in disordered case where the quantum coherence among electrons becomes important. In such case of weak localization the wall can contribute to a decrease of resistivity by causing dephasing. At lower temperature this effect grows and can win over the classical contribution, in particular in wire of diameter $L_\perp \lesssim \ell_\varphi$, ℓ_φ being the inelastic diffusion length. Conductance change of the quantum origin caused by the motion of the wall is also discussed.

I. INTRODUCTION

A. Resistivity in bulk magnetic metals

Since more than a century ago number of studies has been carried out on the electric transport properties in ferromagnetic metals. They revealed many remarkable features which are not seen in non-magnetic metals. One of the most notable phenomena would be the hysteretic and anisotropic behavior of the resistance in the magnetic field (magnetoresistance) observed at small magnetic field of $\lesssim 1$T, which has been already noted more than a hundred years ago [1]. The magnetoresistance in the case of the field H parallel to the current I takes a minimum at a finite value of the field (~ 200Oe for instance for the case of Ni and Fe) . If the field is applied perpendicular to the current, the curve of magnetoresistance is reversed; namely resistivity shows a maximum at certain field and decreases as the field deviates from the value. The hysteretic behavior of the magnetoresistance is due to the fact that the resisitivity is mostly governed by the magnetization M, which corresponds to a field of ~ 1T and thus is larger than the applied magnetic field in the field range we are interested in, except very close to the coercive field where the magnetization vanishes. The observed resistivity ρ as a function of the field, H, has been shown to be well fitted by a phenomenological relation of $\rho \sim \rho_0 + \Delta\rho_{\rm ani} < \cos^2\theta_M >$, where ρ_0 is the field independent part and $\Delta\rho_{\rm ani}$ measures the strength of the anisotropy in the resistivity [2,3] . θ_M is the mutual angle between the local magnetization and the current, which depends on the magnetic field, and bracket denotes the average over the sample. The anisotropy $\Delta\rho_{\rm ani}$ is expressed in terms of the resistivity in the case of the field parallel to the current, $\rho_\parallel$, and that in the perpendicular case, $\rho_\perp$, as $\Delta\rho_{\rm ani} = \rho_\parallel - \rho_\perp$. In most of the ferromagnetic metals $\rho_\parallel$ takes a larger value than $\rho_\perp$; namely $\Delta\rho_{\rm ani}$ is positive [4]. This anisotropic behavior of the resistivity is called anisotropic magnetoresistance (AMR).

A microscopic explanation of AMR has been given by Smit [2] and McGuire and Potter [3] in the following way. They discussed that the conduction (s-) electron is coupled to the magnetization due to the scattered into the magnetic (d-) band and spin-orbit interaction there, and that this process gives rise to an spin asymmetric lifetime, which depends on the angle between the current and the field, resulting in an anisotropy. According to their arguments, positiveness of $\Delta\rho_{\rm ani}$ is explained if the resistivity is dominated by the electron of the minority spin. It was shown recently that the magnitude and the sign of $\Delta\rho_{\rm ani}$ can indeed be controlled by changing the spin asymmetry in scattering in magnetic multilayers, which would support the above explanation [6].

B. Domain wall contribution to classical magnetoresistance

The magnetoresistance observed so far in bulk materials is mostly understood well in terms of AMR effect, which assumes that the magnetization changes very slowly and hence the electron feels only the average magnetization [3].

However this assumption may not be good in real magnets which contains many domains having different direction of the local magnetization. In fact the boundary of these domains is a structure called a domain wall where the spins rotate spatially within a finite distance (Fig. 1). Such domain walls can lead to a scattering of the electron, which is not taken into account in the standard AMR argument. In this paper we exclusively consider the effect of domain walls on the electronic transport properties. Of particular interest would be the case of a small sample less than a typical domain size $\simeq 1 \sim 10\mu$m, since there the magnetic properties can be described in terms of domain wall configuration. In fact in such samples the magnetization process as the field is swept will be described by the nucleation of one or a few domain walls, motion of the walls by depinning followed by the annihilation. If domain walls can have some contribution to the resistivity these dynamics of the wall will appear in the magnetoresistance as discrete jumps in the measurement with the field is swept, since such events are faster (e.g., the speed of domain wall motion is estimated to be about 182m/s in submicron wire of NiFe [7]) compared to the sweep speed. These effects are similar to the Barkhausen noise [8]. Such effect will not be seen very clearly in bulk samples, since there the contribution from many domain walls will be summed up in the observed magnetoresistance and thus the contribution from each domain wall will not be visible. Indeed such jumps in the magnetoresistance has been observed recently in a Ni wire of about the diameter of 300Å [9–12], in submicron [13] and micron size wire of Fe [5,14,15] and Co wires [16,17].

Let us here give a rough estimation of the effect of the wall on the classical electron transport. The most important parameter in doing this is the thickness of the wall, λ, the length in which the spins rotate spatially between the two adjacent domains. This quantity is determined by the competition between the exchange energy per site, J, which aligns the neighboring spins and the magnetic anisotropy energy in the easy axis, K, which tends to make thinner the wall to keep minimum the deviation of spins from the easy axis, as $\lambda = \sqrt{J/K}a$, a being the lattice constant. Thus λ depends on the material and also on the sample shape since K depends on the shape. In the case of $3d$ transition metals such as iron and nickel $\lambda \simeq 500 \sim 1000$Å [10], and $\lambda \sim 150$Å in Co thin film [18]. Hence this is very large compared with the length scale of the electron, $k_F^{-1} \sim O(1\text{Å})$ (k_F being the Fermi wave length of the electron). In such materials, therefore, the conduction electron can adiabatically adjust itself to the local magnetization at every point as it passes through the wall, resulting in a very small scattering probability by the wall. The classical resistivity in the Boltzmann's sense, which is proportional to the reflection probability by the wall, is thus expected to be negligiblly small. This was explicitly shown by Cabrera and Falicov [19] by calculating in the clean limit the reflection coefficient based on the one-dimensional Schrödinger equation for the electron coupled via exchange coupling to the magnetization whose configuration is a domain wall. They obtained for the case of thick wall, $k_F\lambda \gg 1$ the expression $\rho_{\rm w} \propto \exp(-2\pi k_F\lambda)$ for the wall contribution, and discussed that the wall can have large effect only if the wall is extremely thin ($k_F\lambda \lesssim 1$) and if the conduction electron is strongly polarised by the magnetization. In hard magnets with strong magnetic anisotropy as in materials containing rare-earth like $SmCo_5$ and manganese perovskites, λ can be as small as about 10Å. Thus in such systems the resistivity may be dominated by scattering by domain walls, as indicated in recent experiments in the ferromagnetic phase of manganese perovskites [20].

In the past few years there has been a renewal of interest in theory of the classical resistivity due to the domain wall [21–27], because precise measurements of the effects are now becoming possible. It has been pointed out by Levy and Zhang [23] that in the presence of a spin asymmetry in the electron lifetime, which is the case in most ferromagnets, domain wall can have a substantial effect on the classical resistivity by mixing the two spin channels with different resistivity, in agreement with the experiment on Co film [18]. The effect of lifetime asymmetry has been further discussed in detail in ref. [25]. The domain wall resistivity in the ballistic limit has been discussed by use of realistic band structures in ref. [26]. It was shown there that the existence of nearly degenerate bands at the Fermi level in real magnets enhances the classical resistivity due to the wall.

One of systems of recent particluar interest is an atomic scale contact of magnetic metals in the ballistic region. In such narrow contacts the profile of the wall is determined mostly by the shape rather than the anisotropy energy of the bulk magnets, and thus the wall is trapped in a contact region, which is typically nm scale. The adiabaticity does not hold in such cases of small $k_F\lambda$ comparable to 1, and a large effect from the wall is expected [19,26,27]. In fact a magnetoresistance of 200% has been observed in ballistic Ni nanocontacts where the number of the channel is less than $N \lesssim 10$ [28], and this has been interpreted in terms of a strong reflection by a nanometer scale domain wall [27]. Ballistic nano-contacts would be one of the novel systems in which a large magneto-electronic effect is expected. In the dirty case in contrast, the effect is not so large, since the wall scattering is smeared out by impurity scattering [27].

Intensive studies has been carried out experimentaly on sub-micron scale wires [9–15,**?**,17,29]. These are explained in detail in §I E. A structure of layers of hard and soft ferromagnets would be an interesting possibility to investigate the effect of the domain wall, since there the thickness of the wall can be controlled by the external magnetic field as carried out in ref. [30]. Measurement of conductance through a sub-micron ferromagnetic dot on a semi-conductor wire has been carried out [31]. Semi-conductors are interesting since the electron can feel a larger coupling to the wall

can be larger due to a larger electron Fermi wavelength compared with metals.

C. Quantum transport

So far these studies both experimentally and theoretically are carried out mostly in the case of low resistivity materials, where the transport can be discussed in terms of the classical theory. However besides the classical transport, there is another important aspect in electronic transport at low temperature. This is the effect of the quantum coherence among electrons, which modifies the low energy electronic properties significantly. The effect becomes important in disordered metals with high resistivity, where the elastic mean free path becomes shorter due to the elastic impurities, which cause only elastic scattering. The electron wave scattered by such normal impurities can interfere with the incoming wave, leading to a state like a standing wave. This is called weak localization and the resistivity in this case is enhanced due to the quantum interference [32,33]. This correction becomes large in low dimensions such as in wires since there the interference becomes stronger. The interesting point of this situation is that the electronic properties are very sensitive to a small disturbance because of the presence of coherence. For instance in a non-magnetic metals of micron size, even a motion of a *single* impurity atom has been shown to change at low temperature the conductance ($G \equiv \sigma A_\perp/L$, $A_\perp$ and L being the crossssectional area and the length of the system) of the entire system by disturbing the coherence [34]. The magnitude of the conductance change turns out in most cases to be a universal order of e^2/h [35]. It is then reasonable to expect that in mesoscopic ferromagnetic metals, domain walls can lead to a large change of conductance in the presence of quantum interference. In fact this possibility has been pointed out in ref. [22]. The most remarkable point is that because a domain wall destroys the interference among the electron, the wall contributes to a negative quantum correction to the resistivity. In disordered $3d$ transition metals, this quantum correction can win over the classical contribution, and thus a nucleation of a wall in the sample may lead to a *decrease* of resistivity. A recent numerical simulation also supports the negative resistivity contribution from the wall in disordered thin wire [36]. Recently it has been pointed out that the geometric phase attached to the electron spin as it passes through the wall can also cause important dephasing effect, which would become important in multiply connected geometry [37,38]. The effect of dephasing due to the magnetic origin has been considered also in the thin film of metal sandwiched by ferromagnetic layers. There the internal magnetic field at the interface causes dephasing in the conduction layer in the presence of the spin-orbit scattering, which contributes to a positive magnetoresistance [39].

In real materials there are source of dephasing other than such magnetic objects, such as phonons, electron-electron interaction [32,33]. In magnets the fluctuation of the magnetization, i.e., spin wave, also contributes to the dephasing. Such effects can be avoided by observing at low termperature. In bulk or film of ferromagnetic metals, the existence of strong internal field of about 1T can also destroy the coherence [32,33]. Fortunately this is not the case in a narrow wire as discussed in §IV A.

Quite recently experimental efforts in search for the quantum coherence in magnetic metals have been carried out [40]. The resistivity of a Co wire of 1000Å width which contains a loop of 500nm has been studied in ref. [40]. It was argued there that from the absence of Aharaonov-Bohm oscillations the phase-breaking length of the Co at $T = 0.29$K is shorter than 0.3μm. The study of a ferromagnetic single electron transistor of double Ni/NiO/Co tunnel junctions at 20mK has revealed that higher order tunneling processes dominate in the Coulomb blockade region, in which two or more electrons coherently tunnels through the two junctions [41]. This result suggests the electronic coherence is kept there for $\sim 2.5\mu$m, which is the length of the Co island.

Because of its sensitivity these conductance fluctuation as a consequence of quantum interference has already been used as a probe in the studies of various mesoscopic metallic or semi-conducting systems. For example a telegraph noise due to a two-level oscillation of a defect in Bi film has been investigated and it turned out that the oscillation at $T \lesssim 1$K is governed by the quantum tunneling subject to the dissipation from the conduction electron [42]. Such measurement of the quantum transport properties has been proved to be a useful probe also for studies of mesoscopic spin-glass systems [43,44] and the magnetization flip of mesoscopic magnets [45].

D. Mesoscopic magnets

Quite recently the resistivity measurements has been carried out to investigate the the reversal of the magnetization in mesoscopic magnets at low temperature [9–13,**?**,15–17,29–31]. They are motivated by the interest in the magnetization reversal via quantum fluctuation of magnetization [46]. In the case of very small magnets this process of magnetization flip is expected to be well described by the uniform rotation of the total magnetization. At high temperature and in bulk magnets these processes are caused by the thermal activation over the energy barriers due

to the anisotropy energy, nucleation energy or the pinning potential. If the thermal activation is the only process of magnetization reversal, a freezing of the magnetization is expected in the limit of zero temperature. However, particles of nanometer size have a finite quantum fluctuation, although it is not very large in large magnets compared to the atomic scale. Thus another process of a magnetization flip is possible, *i.e.*, via a quantum tunneling, leading to a finite relaxation rate even at zero temperature [47,46]. The tunneling entity, the total magnetization in nanoscale magnets, are macroscopic or semimacroscopic objects compared to the atomic scale, and thus these tunnelings are called a macroscopic quantum tunneling (MQT) [48]. Assuming the case of very small magnets, the theories so far are based on a simplified picture of the relaxation being described by a single variable which tunnels through a single energy barrier. Then the relaxation expected will depend exponentially on time, $M \propto \exp(-\Gamma t)$ (Γ being the decay rate). Many experimental attempts has been made in search for such quantum tunneling of magnetization for about a decade [46]. In the studies at the beginning of the 90's the the relaxation of the magnetization of small ferromagnetic particles whose diameters are about $40 \sim 150$Å has been measured by use of SQUID (superconducting quantum interference device) [49,50]. Because the sensitivity of the SQUID used was not so high, only a collection of many particles could be measured. The observed relaxation was logarithmic in a wide range of the time, $M \sim S_{\rm v} \ln t$, where $S_{\rm v}$ is a constant called the magnetic viscosity, in contrast to the exponential dependence predicted by simple theories. This discrepancy would be due to the distribution of the size and shape of the particles. A tendency of saturation of $S_{\rm v}$ to a finite value as temperature decreases has been reported, but because the size distribution is unknown, no definite conclusion could be drawn concerning whether the relaxation is really of the quantum origin or not.

Recent experiments thus aim at observation of relaxation without any ambiguity in the interpretation. A first such possibility would be to use better samples. For example, magnetic molecules are good candidates because of their uniform structure. In fact a crystal of Mn_{12} acetate, made up of molecules containing twelve manganese atoms which form the total spin of $S = 10$, has been shown to exhibit the exponential decay of magnetization [51] consistent with the picture of a single energy barrier [47]. The data clearly showed that the decay is due to the quantum tunneling below 2K. Further study on the system revealed the resonant tunneling in each molecule [52]. These behavior consistent with a picture of a tunneling of the total magnetization through a single energy barrier may be natural because the spin which tunnels, $S = 10$, is microscopic rather than mesoscopic. Magnets of biological origin is another candidate for definitive experiments. For example the AC susceptibility has been measured on ferritine particles from horse spleen, each particle is spherical and contains a cluster of antiferromagnetically coupled Fe atoms, the diameter being 75Å [53]. The imaginary part of the susceptibility showed a sharp peak at about 1MHz, which may to be explained by the resonance with the coherent oscillation of the magnetization due to the quantum tunneling, namely a macroscopic quantum coherence. Although there has been some arguments concerning the interpretation [54], further studies on samples with different diameter indicates the above explanation would be correct [55,56].

As a second approach to a definitive experiments, direct observation of the magnetization of a single nanoscale magnet has recently been carried out. Magnetic force microscope (MFM) [57] and micro-SQUID [58] has been used to study the reversal of the magnetization of a small particle of γ-Fe_2O_3 with the size of 3000Å at room temperature and of 800Å Co particle at low temperature. It turned out that even for such a small particle the relaxation is logarithmic in time, which is argued to be due to pinning by inherent defects and surfaces [57,59]. Indeed recent measurement on a smaller particle of $150 \sim 300$Å indicates the uniform rotation of the magnetization [60]. In the observed temperature range of $0.2 < T < 6$K, however, there was no indication of quantum tunneling.

In the case of wires, the nucleation, depinning and annihilation of domain walls can be driven by the quantum fluctuation [61,62]. Intensive efforts has been put for experimental confirmation on Ni wires of width of $300 \sim 400$Å by use of resistivity measurements [9–11]. These earlier works seemed to suggest the depinning by quantum tunneling below 5K [9–11], but in the SQUID measurement of a 650Å wire no evidence of quantum tunneling has been found in the temperature range of $0.1 \sim 6$K [63]. It has been, however, indicated in the observation of the response to the microwave that the energy levels of a pinned wall is quantized [11]. Another possibility of tunneling of the chirality of the domain wall, i.e., the way the magnetization rotates inside the wall, has been discussed in Refs. [64,65].

E. Resistivity measurements of magnetic wires

For studies of the magnetic behaviors of nanoscale metallic magnets, electronic transport measurement can be effective because of its sensitivity and facility. In fact a telegraph noise measurement of an antiferromagnetically coupled small cluster of ErAs on GaAs, where the diameter of the clusters are estimated to be about 30Å has been carried out [45]. It was shown that the telegraph noise was due to a flip of a magnetization of each cluster, the magnitude being $\sim 41 \sim 150\mu_B$. Result indicated that the flip is due to the tunneling below 350mK. Transport measurements are particularly useful in magnetic wires. The measurement of the magnetoresistance of a Ni wire with diameter of $200 \sim 400$Åwith the length of $\sim 10\mu$m has revealed a discrete jump of the resistivity as the magnetic field

along the wire direction is swept at temperature of $1.4 \sim 22$K [9,10]. The global curve of magnetoresistance observed there was similar to the behavior of positive magnetoresistance common in bulk ferromagnetic metals [3]. The jump appeared close to the minimum of the resistivity and was reproducible except for a slight distribution of the value of the field at which the jump occurs. The magnitude was about 0.02% of the total resistivity. It was argued there that the jump would be due to the change of the average magnetization associated with the depinning of a domain wall. The explanation of this jump by use of the conventional AMR [3] has been given there and the displacement of the wall was estimated from the magnitude of the jump to be about 1.2μm. They argued from the distribution of the position of the jump that the depinning is dominated by quantum tunneling below 5K [10], but another measurement on 650Å carried out by use of SQUID has found only process of thermal activation down to 0.13K [63]. Recently similar experiment was carried out on Fe wire with width of 3000Å and there two reproducible jumps in the resistivity have been observed at 0.3K, negative jump followed by a positive one as the field increases [13]. The first and second jump are expected to be due to the nucleation and annihilation of a domain wall, respectively, and then the resistivity seems to be suppressed by the wall. This decrease of resistivity by the wall is expected when the coherence among electrons is important [22]. Other recent measurements on sub-micron scale wires also suggest a negative contribution of the wall at low temperature [12,17]. These samples are dirty with the residual resistivity of about $\rho_0 \sim 10\mu\Omega$cm. Negative contribution has also been seen in cleaner sample of Fe with $\rho_0 \sim 0.2\mu\Omega$cm [14]. These effects have been observed to grow at lower temperature (below 50K [14] and 20K [17]). These behaviors might be considered as an experimental confirmation of the quantum coherence effect predicted in ref. [22], although further detailed studies are obviously needed. For instance the temperature of 20K seems to be rather high for the weak localization correction to be important, especially for the clean case of ref. [14]. A classical origin of negative contribution from the wall, arising from the effect of the surface, has been suggested in ref. [15]. Thus at present the reduction of the resistivity due to the wall observed in wires at low temperature is not fully understood. In contrast, at room temperature, the existence of the walls has been shown to enhance the resistivity in wires [29] and films [18], which is interpreted as classical process of reflection with the lifetime asymmetry taken into account [23].

In order to give an definitive interpretation for such discrete jumps in the magnetoresistance, calculation of the resistivity in the presence of a domain wall based on a microscopic consideration which takes into account various effect such as AMR, the quantum correction and the spin asymmetry is necessary. In this paper we focus on the effect of the quantum correction, since it can be especially interesting because of a substantial enhancement of the effect of the wall expected in low dimension and at low temperature. A resistivity measurement in the weakly localized regime of the electron is expected to be a powerful tool for studies of nanoscale magnets at low temperature.

This paper is organized as follows. In section II the classical resistivity due to a domain wall in the Boltzmann's sense is calculated based on the theory of linear response taking account the impurity scattering at the same time. The electron is treated as in three-dimensions since in actual wires the diameter $L_\perp$ would be large enough, $L_\perp \gg k_F^{-1}$. The wall is treated as flat which is justified if $L_\perp \lesssim \lambda$. The interaction between the conduction electron and the magnetization is the exchange coupling. We rewrite the system by use of a local gauge transformation which makes the z-axis of the electron spin chosen always along the local magnetization. The wall is then expressed by a classical gauge field, if the reaction from the electron on the wall is neglected. The effect of the wall is taken into account up to the second order. In section III the quantum correction to the resistivity is discussed. The quantum correction becomes important when there is enough scattering by disorder, which causes the interference between the scattered and unscattered electron waves, leading to weakly localized states of the electron. This interference effect is expressed by a particle-particle ladder (Cooperon), which is singular at small momentum transfer. The domain wall in ferromagnetic metals turns out to give rise to a mass in the Cooperon, thus it suppresses the localization. The resistivity will, therefore, decrease when a domain wall is nucleated, in contrast to naive classical intuition. The effect would be particularly important in narrow wires. The resistivity change due to the motion of the wall is discussed in section V. The case of weakly localized electron system is considered since there the effect will be much larger than that expected from the classical argument based of the anisotropic magnetoresistance. Summary is given in section VI. Details of calculation is given in Appendices. This paper is an extended and detailed paper of the letter published before [22].

II. CLASSICAL RESISTIVITY DUE TO A DOMAIN WALL

We consider here the case of the s-d model where the conduction electron, c, couples to a localized spin, $\boldsymbol{S}$, by exchange coupling, the coupling constant being g. The Lagrangian of the electron in the imaginary time (denoted by τ) is then written as

$$L = \sum_{\mathbf{k}\sigma} c^\dagger_{\mathbf{k}\sigma}(\partial_\tau + \epsilon_{\mathbf{k}})c_{\mathbf{k}\sigma} - g\int d^3x \boldsymbol{S}(\mathbf{x})(c^\dagger \boldsymbol{\sigma} c) + H_{\rm imp}, \tag{1}$$

where $\epsilon_{\mathbf{k}} \equiv \hbar^2\mathbf{k}^2/2m - \epsilon_F$ (ϵ_F being the Fermi energy). The spin index is denoted by $\sigma = \pm$ and $\boldsymbol{\sigma}$ is the Pauli matrix. The last term describes the interaction between the electron and the impurity:

$$H_{\rm imp} \equiv v \sum_{\mathbf{k},\mathbf{q}} \sum_{i=1}^{n_{\rm i}} e^{i\mathbf{q}\cdot\mathbf{X}_i} c^\dagger_{\mathbf{k}+\mathbf{q}} c_{\mathbf{k}}, \tag{2}$$

where v is the coupling constant and $\mathbf{X}_i$'s are the position of the impurities which is assumed to be random, $n_{\rm i}$ being the number of impurities. Due to this interaction the electron has a finite elastic lifetime, $\tau \equiv \hbar/[2\pi n_{\rm i} v^2 N(0)]$, $N(0) \equiv Vmk_F/2\pi^2\hbar^2$ being density of states at Fermi energy (V is the system volume). Here we assume the same lifetime for electron with both majority and minority spin. The effect of the lifetime difference has been discussed in Refs. [23–25].

In the case of the system described by a single-band model, it can be shown in the Hartree-Fock approximation that the effective Lagrangian describing the low energy behavior of the electron and the magnetization is the same as eq. (1) with g replaced by the Coulomb repulsion, U, but then the exchange coupling J below is determined by U [62]. The Lagrangian (1) can describe both s and d electron if g and thus the splitting (Δ) below is appropriately chosen.

The configuration of the localized spin is determined by the ferromagnetic Heisenberg model,

$$H_S = \int d^3x \left[\frac{J}{2} |\nabla \boldsymbol{S}|^2 - \frac{K}{2} S_z^2 + \frac{K_\perp}{2} S_x^2 \right], \tag{3}$$

where J is the effective exchange energy and K and $K_\perp$ are the magnetic anisotropy energy introduced phenomenologically, which are assumed to include the effect of the demagnetization field. The transverse anisotropy energy, $K_\perp$, which determines the inertial mass of the wall, does not affect our calculation of a static wall. It becomes essential in discussing the dynamics of the magnetization such as the tunneling of the chirality [64,65].

Here we are interested in the solution of a single domain wall. In terms of the polar coordinates, (θ, ϕ), that represents the direction of $\boldsymbol{S}$, the solution of a domain wall at $z = z_0$ is given by

$$\cos\theta = \tanh\frac{z - z_0}{\lambda}, \quad \phi = \pm\frac{\pi}{2}. \tag{4}$$

Here $\lambda = \sqrt{K/J}$ is the thickness of the wall. The configuration is depicted in Fig. 1.

In eq. (1) the last term represents the interaction between the local spin and the electron. This term, however, contains the interaction, which exists even far from the wall, and so does not lead to the scattering of the electron. Thus we need to rewrite this interaction to the form appropriate for the perturbative calculation of resistivity. This can be carried out by use of the local gauge transformation which rotates the spin axis of the electron so that the z-axis is always along the local direction of the localized spin $\boldsymbol{S}$. Explicitly this transformation is given by

$$a_\sigma = \sigma \cos\frac{\theta}{2}\, c_\sigma + e^{-i\sigma\phi} \sin\frac{\theta}{2}\, c_{-\sigma}. \tag{5}$$

In terms of the new electron operator, a, the Lagrangian is written as [62]

$$L = \sum_{\mathbf{k}\sigma} a^\dagger_{\mathbf{k}\sigma} (\partial_\tau + \epsilon_{\mathbf{k}\sigma}) a_{\mathbf{k}\sigma} + H_{\rm int} + H_{\rm imp}, \tag{6}$$

where

$$\epsilon_{\mathbf{k}\sigma} \equiv \epsilon_{\mathbf{k}} - \sigma\Delta \tag{7}$$

is the energy of the electron polarised in z-direction by the magnetization with $\Delta \equiv g|\boldsymbol{S}|$ being half the splitting between the up and down spin electrons. The term $H_{\rm int}$ describes the interaction between the electron and the wall and is given by

$$\begin{aligned} H_{\rm int} &\equiv \frac{\hbar^2}{2m} \int d^3x \left[\frac{1}{2} \sum_\pm \mp e^{\mp i\phi} \nabla_z\theta (a^\dagger \sigma_\pm \overset{\leftrightarrow}{\nabla}_z a) + \frac{1}{4} (\nabla_z\theta)^2 (a^\dagger \sigma_x a) \right] \\ &= \frac{\hbar^2}{2m} \sum_{\mathbf{k}} \sum_{q//z} \left[\sum_\pm \mp i e^{\mp i\phi} \left(k_z + \frac{q}{2} \right) A_q a^\dagger_{\mathbf{k}+q} \sigma_\pm a_{\mathbf{k}} + \frac{1}{4} \sum_{p//z} A_p A_{-p+q} a^\dagger_{\mathbf{k}+q} a_{\mathbf{k}} \right]. \end{aligned} \tag{8}$$

Here $(a^\dagger \overleftrightarrow{\nabla} a) \equiv a^\dagger(\nabla a) - (\nabla a^\dagger)a$,

$$A_{\mathbf{q}} \equiv \frac{1}{V}\int d^3x e^{-iqz}\nabla_z\theta = \frac{\pi}{L}e^{-iqz_0}\frac{1}{\cosh(\pi q\lambda/2)}\delta_{\mathbf{q}_\perp,0} \tag{9}$$

is a classical gauge field which represents the domain wall, $V \equiv L_\perp^2 L$ being the system volume and $\mathbf{q} \equiv (\mathbf{q}_\perp, q)$, $\mathbf{q}_\perp$ being the momentum in xy-plane and q is along z-direction. A_q is finite only when $\mathbf{q}_\perp = 0$, since we are considering a flat wall perpendicular to the z-axis. Below we choose $\phi = \pi/2$. We neglect the reaction to the wall from the conduction electron, since the wall is much heavier than the electron, and then the gauge field a_q can be treated as a classical variable independent of time. Due to this gauge transformation, the electronic current in z-direction is changed to be

$$J_z \equiv -\int d^3x \frac{e\hbar}{m}\frac{i}{2}(c^\dagger \overleftrightarrow{\nabla}_z c) = J_z^0 + \delta J, \tag{10}$$

where

$$J_z^0 \equiv \frac{e\hbar}{m}\sum_{\mathbf{k}} k_z a_{\mathbf{k}}^\dagger a_{\mathbf{k}} \tag{11}$$

is the usual current and there arises and additional current carried by the wall,

$$\delta J \equiv -\frac{e\hbar}{2m}\sum_{\mathbf{k},q//z} A_q a_{\mathbf{k}+q}^\dagger \sigma_x a_{\mathbf{k}}. \tag{12}$$

A. Disordered case

We first consider a disordered case where the resistivity is dominated by normal impurities. The effect of the wall is calculated perturbatively based on Kubo formula. The conductivity σ for the current along the wire is calculated from the imaginary current-current correlation function

$$Q(i\omega_\ell) \equiv \frac{\hbar}{V} < J_z(i\omega_\ell)J_z(-i\omega_\ell) >, \tag{13}$$

where $\omega_\ell \equiv 2\pi\ell/\beta$ being the Matsubara frequency and $\beta \equiv 1/(k_B T)$) as (we define the Fourier transform of the electron as $a_n \equiv (1/\sqrt{\beta})\int_0^\beta d\tau e^{i\omega_n\tau}a(\tau)$)

$$\sigma = \lim_{\omega\to 0}\mathrm{Im}(Q(\hbar\omega + i0) - Q(i0))/\omega. \tag{14}$$

Here $Q(\hbar\omega + i0)$ is the retarded correlation function obtained by analytical continuation, $Q(\hbar\omega + i0) \equiv Q(i\omega_\ell \to \hbar\omega + i0)$, and Im denotes the imaginary part. We estimate the correction to the conductivity due to the wall to the second order of A_q. In this section we consider only the correction to the classical (Boltzmann) conductivity (σ_c). The quantum corrections represented by maximally crossed diagrams are considered in §III.

Zeroth order term of Q is obtained as $Q_0(i\omega_\ell) = -(e\hbar/m)^2(\hbar/V\beta)\sum_{n\mathbf{k}\sigma} k_z^2 G_{\mathbf{k}n\sigma}G_{\mathbf{k},n+\ell,\sigma}$ and this leads to a well know classical conductivity due to the normal impurity, $\sigma_0 \equiv e^2 n\tau/m$ (n being the electron density). Here the imaginary time electron Green function includes the effect of the impurity and is given by

$$G_{\mathbf{k},n,\sigma} \equiv \frac{1}{i(\omega_n + \frac{\hbar}{2\tau}\mathrm{sgn}(n)) - \epsilon_{\mathbf{k}\sigma}}, \tag{15}$$

where $\omega_n \equiv \pi(2n-1)/\beta$ and $\mathrm{sgn}(n) = 1$ and -1 for $n > 0$ and $n < 0$, respectively. Green function carrying a frequency of $\omega_n + \omega_\ell$ is denoted by $G_{\mathbf{k},n+\ell,\sigma}$.

The first order contribution of A_q vanishes. The second order contributions to the Boltzmann conductivity are shown in Fig. 2. The process Q_1 arises from the correction of the both of the two current vertices by the wall, δJ, and Q_3 is due to the correction of one of the current vertex and a interaction with the wall. Q_2 and Q_4 are the self-energy due to the wall and Q_5 is the vertex correction. These are written as

$$
\begin{aligned}
Q_1 &= -\left(\frac{e\hbar}{m}\right)^2 \frac{1}{4}\frac{1}{\beta}\sum_n \frac{1}{V}\sum_{\mathbf{k}q\sigma} |A_q|^2 G_{\mathbf{k}-\frac{q}{2},n,\sigma} G_{\mathbf{k}+\frac{q}{2},n+\ell,-\sigma} \\
Q_2 &= -\left(\frac{e\hbar}{m}\right)^2 \frac{\hbar^2}{8m}\frac{1}{\beta}\sum_n \frac{1}{V}\sum_{\mathbf{k}q\sigma} k_z^2 |A_q|^2 [(G_{\mathbf{k},n,\sigma})^2 G_{\mathbf{k},n+\ell,\sigma} + G_{\mathbf{k},n,\sigma}(G_{\mathbf{k},n+\ell,\sigma})^2] \\
Q_3 &= -\left(\frac{e\hbar}{m}\right)^2 \frac{\hbar^2}{2m}\frac{1}{\beta}\sum_n \frac{1}{V}\sum_{\mathbf{k}q\sigma} k_z\left(k_z-\frac{q}{2}\right) |A_q|^2 [G_{\mathbf{k}-\frac{q}{2},n,\sigma} G_{\mathbf{k}-\frac{q}{2},n+\ell,\sigma} G_{\mathbf{k}+\frac{q}{2},n,-\sigma} \\
&\quad + G_{\mathbf{k}-\frac{q}{2},n,\sigma} G_{\mathbf{k}-\frac{q}{2},n+\ell,\sigma} G_{\mathbf{k}+\frac{q}{2},n+\ell,-\sigma}] \\
Q_4 &= -\left(\frac{e\hbar}{m}\right)^2 \frac{\hbar^4}{4m^2}\frac{1}{\beta}\sum_n \frac{1}{V}\sum_{\mathbf{k}q\sigma} k_z^2\left(k_z-\frac{q}{2}\right)^2 |A_q|^2 [(G_{\mathbf{k}-\frac{q}{2},n,\sigma})^2 G_{\mathbf{k}-\frac{q}{2},n+\ell,\sigma} G_{\mathbf{k}+\frac{q}{2},n,-\sigma} \\
&\quad + G_{\mathbf{k}-\frac{q}{2},n,\sigma}(G_{\mathbf{k}-\frac{q}{2},n+\ell,\sigma})^2 G_{\mathbf{k}+\frac{q}{2},n+\ell,-\sigma}] \\
Q_5 &= -\left(\frac{e\hbar}{m}\right)^2 \frac{\hbar^4}{4m^2}\frac{1}{\beta}\sum_n \frac{1}{V}\sum_{\mathbf{k}q\sigma} k_z^2\left(k_z^2-\frac{q^2}{4}\right) |A_q|^2 G_{\mathbf{k}-\frac{q}{2},n,\sigma} G_{\mathbf{k}-\frac{q}{2},n+\ell,\sigma} G_{\mathbf{k}+\frac{q}{2},n,-\sigma} G_{\mathbf{k}+\frac{q}{2},n+\ell,-\sigma}.
\end{aligned}
\tag{16}
$$

The contribution from the wall needs to vanish in the limit of vanishing Zeeman splitting, $\Delta \to 0$, since no scattering occurs. This is not easy to see by looking at each term, Q_i, but it will become obvious after we sum up these classical contributions to be $Q_{1-5} \equiv \sum_{i=1,5} Q_i$. In fact the summation can be carried out in a straight forward manner by use of identities

$$
\begin{aligned}
G_{\mathbf{k},n,\sigma} G_{\mathbf{k},n+\ell,\sigma} &= -i\left(\omega_\ell + \frac{\hbar}{2\tau}(\mathrm{sgn}(n+\ell) - \mathrm{sgn}(n))\right)^{-1} (G_{\mathbf{k},n,\sigma} - G_{\mathbf{k},n+\ell,\sigma}) \\
G_{\mathbf{k}+\frac{q}{2},n,-\sigma} G_{\mathbf{k}-\frac{q}{2},n,\sigma} &= \left(\frac{\hbar^2 k_z q}{m} + 2\sigma\Delta\right)^{-1} (G_{\mathbf{k}+\frac{q}{2},n,-\sigma} - G_{\mathbf{k}-\frac{q}{2},n,\sigma}).
\end{aligned}
\tag{17}
$$

The result is (see Appendix A for details of calculation) $Q_{1-5} = Q_{\rm c} + Q'_{\rm c}$, where

$$
Q_{\rm c}(i\omega_\ell) = \frac{1}{2}\left(\frac{e\hbar\Delta}{m}\right)^2 \frac{1}{\beta}\sum_n \frac{1}{V}\sum_{\mathbf{k}q\sigma} |A_q|^2 G_{\mathbf{k}-\frac{q}{2},n,\sigma} G_{\mathbf{k}-\frac{q}{2},n+\ell,\sigma} G_{\mathbf{k}+\frac{q}{2},n,-\sigma} G_{\mathbf{k}+\frac{q}{2},n+\ell,-\sigma},
\tag{18}
$$

and

$$
Q'_{\rm c}(i\omega_\ell) = -\frac{1}{4}\left(\frac{e\hbar}{m}\right)^2 \frac{1}{\beta}\sum_n \frac{1}{V}\sum_{\mathbf{k}q\sigma} |A_q|^2 \Delta \frac{\Delta - \sigma\frac{(k_z+q/2)^2}{m}}{\left[\Delta + \sigma\frac{(k_z+q/2)q}{2m}\right]^2} G_{\mathbf{k},n,\sigma} G_{\mathbf{k},n+\ell,\sigma}.
\tag{19}
$$

The term $Q_{\rm c}$ is dominant and the contribution from the term $Q'_{\rm c}$ turns out to cancel with the effect of the shift of the electron density, which is calculated later.

The summation over Matsubara frequency, ω_n, in eqs. (18) and (19) can be carried out by use of contour integration (see Appendix C) and the contribution to the Boltzmann conductivity from the five classical processes, $\sigma_{1-5} \equiv \lim_{\omega\to 0} \mathrm{Im}(Q_{1-5}(\omega + i0) - Q_{\rm c}(i0))/\omega$, is obtained as $\sigma_{1-5} = \sigma_{\rm c} + \sigma'_{\rm c}$, where

$$
\sigma_{\rm c} = -\frac{\Delta^2\hbar^3}{8\pi\tau^2}\left(\frac{e\hbar}{m}\right)^2 \frac{1}{V}\sum_{\mathbf{k}q\sigma} |A_q|^2 \frac{(\epsilon_{\mathbf{k}-\frac{q}{2},\sigma} + \epsilon_{\mathbf{k}+\frac{q}{2},-\sigma})^2}{\left[(\epsilon_{\mathbf{k}-\frac{q}{2},\sigma})^2 + \left(\frac{\hbar}{2\tau}\right)^2\right]^2 \left[(\epsilon_{\mathbf{k}+\frac{q}{2},-\sigma})^2 + \left(\frac{\hbar}{2\tau}\right)^2\right]^2},
\tag{20}
$$

and $\sigma'_{\rm c}$ is the contribution from $Q'_{\rm c}$;

$$
\sigma'_{\rm c} = \frac{\hbar}{32\pi}\left(\frac{e\hbar}{m}\right)^2 \frac{\Delta}{\tau^2}\frac{1}{V}\sum_{\mathbf{k}q\sigma} \frac{|A_q|^2}{\left[\epsilon^2_{\mathbf{k}\sigma} + \left(\frac{\hbar}{2\tau}\right)^2\right]^2} \frac{\Delta - \sigma\frac{(k_z+q/2)^2}{m}}{\left[\Delta + \sigma\frac{(k_z+q/2)q}{2m}\right]^2}.
\tag{21}
$$

Besides the processes in Fig. 2, there is another contribution the classical conductivity, which is due to the change of the electron density in the presence of a domain wall. The correction to the electron density due to the interaction (8) is written as (diagramatically shown in Fig. 3)

$$\delta n = \frac{\hbar^2}{4m}\frac{1}{\beta V}\sum_{\mathbf{k}qn\sigma}|A_q|^2\left[\frac{1}{2}(G_{\mathbf{k}n\sigma})^2 + \frac{\hbar^2 k_z^2}{m}(G_{\mathbf{k}-\frac{q}{2},n\sigma})^2 G_{\mathbf{k}+\frac{q}{2},n,-\sigma}\right]. \tag{22}$$

After some calculation it reduces to (Appendix B)

$$\delta n = -\frac{\hbar^3}{16\pi m\tau}\frac{1}{V}\sum_{\mathbf{k}q\sigma}\frac{|A_q|^2}{\epsilon_{\mathbf{k}\sigma}^2 + \left(\frac{\hbar}{2\tau}\right)^2}\frac{\Delta - \sigma\frac{(k_z+q/2)k_z}{m}}{\Delta + \sigma\frac{(k_z+q/2)q}{2m}}. \tag{23}$$

this shift of the electron density leads to a correction of the zeroth order conductivity, $\sigma_0 \to \sigma_0 + \delta\sigma_{\rm c}$, where $\delta\sigma_{\rm c} = e^2\tau\delta n/m$ is obtained from eq. (23) as

$$\delta\sigma_{\rm c} = -\frac{\hbar}{16\pi}\left(\frac{e\hbar}{m}\right)^2\frac{1}{V}\sum_{\mathbf{k}q\sigma}\frac{|A_q|^2}{\epsilon_{\mathbf{k}\sigma}^2 + \left(\frac{\hbar}{2\tau}\right)^2}\frac{\Delta - \sigma\frac{(k_z+q/2)k_z}{m}}{\Delta + \sigma\frac{(k_z+q/2)q}{2m}}. \tag{24}$$

It turns out after the $\mathbf{k}$-summation that $\sigma_{\rm c}' + \delta\sigma_{\rm c}$ vanishes in the case of $k_F\lambda \gg 1$ (AppendixB). Thus the classical correction to the conductivity due to the wall is given by $\sigma_{\rm c}$.

To proceed further we neglect quantities of $O((q/k_F)^2)$ and approximate $\epsilon_{\mathbf{k}\pm q/2,\mp\sigma} \simeq \epsilon_{\mathbf{k}} \pm [(\hbar^2 k_z q/2m) + \sigma\Delta]$. This is because the momentum transfer, q, is limited to a small value of $q \lesssim \lambda^{-1}$ due to the form factor of the wall, $|A_q|^2 \propto [\cosh(\pi q\lambda/2)]^{-2}$, and we are considering the case of a thick wall, $k_F\lambda \gg 1$. The result of $\mathbf{k}$-summation is (see Appendix D)

$$\sigma_{\rm c} = -\frac{e^2\Delta^2\tau^2}{8\pi\hbar^3}n_{\rm w}\sum_\sigma\int_{-\infty}^{\infty}\frac{dx}{x}\frac{1}{\cosh^2 x}\left[\tan^{-1}\left(\frac{2l_\sigma}{\pi\lambda}x + 2\Delta\frac{\tau}{\hbar}\right) + \tan^{-1}\left(\frac{2l_\sigma}{\pi\lambda}x - 2\Delta\frac{\tau}{\hbar}\right)\right], \tag{25}$$

where $x \equiv \pi q\lambda/2$ and $l_\sigma \equiv \hbar k_{F\sigma}\tau/m$ is the mean free path of the electron with spin σ, $n_{\rm w} \equiv 1/L$ being the density of the wall.

Using this result the contribution of the wall to the Boltzmann resistivity is given as

$$\rho_{\rm c} \equiv (\sigma_0 + \sigma_{\rm c})^{-1} - \sigma_0^{-1} \simeq \frac{|\sigma_{\rm c}|}{\sigma_0^2}. \tag{26}$$

The last expression is valid if the contribution from the impurity is much larger than that from the wall, namely if $|\sigma_{\rm c}|/\sigma_0 \ll 1$. (But see also the discussion below eq. (38))

Here we consider the case of a ferromagnet with weak disorder, and assume two further conditions;

$$\Delta\tau/\hbar \gg 1, \tag{27}$$

which indicates that the effect of Zeeman splitting is not smeared by the width of energy level, and

$$m\Delta\lambda/k_F\hbar^2 \gg 1. \tag{28}$$

The second condition is satisfied if the Zeeman splitting is not too small. Both inequalities would be satisfied in the case of d electron. In this case the classical correction due to the wall is obtained as (eq. (D10))

$$\sigma_{\rm c} \simeq -\frac{e^2}{4\pi^2\hbar}n_{\rm w}\sum_\sigma\frac{l_\sigma}{\lambda}\int_0^\infty\frac{dx}{\cosh^2 x} = -\frac{e^2}{4\pi^2\hbar}n_{\rm w}\sum_\sigma\frac{l_\sigma}{\lambda} \qquad (\Delta\tau/\hbar \gg 1, m\Delta\lambda/k_F\hbar^2 \gg 1). \tag{29}$$

B. Ballistic limit

The ballistic limit, $l \to \infty$, is also of recent interest, as a large magnetoresistance is expected there as is indeed realized in nano scale contacts [28]. In this limit the perturbative calculation with respect to domain wall contribution relative to the normal impurity scattering based on Kubo formula fails. In this case Mori formula becomes valid, which relates the resistivity with the correlation of random forces as [66]

$$\rho_{\rm c} = \left(\frac{e^2 n}{m}\right)^{-2}\lim_{\omega\to 0}\frac{1}{\hbar\omega}{\rm Im}[\chi_{jj}(\hbar\omega) - \chi_{jj}(0)]. \tag{30}$$

Here $\chi_{jj}(i\omega_\ell) \equiv -(\hbar/V) < \dot{J}(i\omega_\ell)\dot{J}(-i\omega_\ell) >$ with $\dot{J} \equiv dJ/dt = \frac{i}{\hbar}[H, J]$. $\omega_\ell \equiv 2\pi\ell/\beta$ is a Bosonic Matsubara frequency ($\beta \equiv 1/(k_B T)$). The correlation function $\chi_{jj}(\hbar\omega)$ in eq. (30) denotes an analytical continuation of the correlation function calculated for imaginary-time frequency, i.e., $\chi_{jj}(\hbar\omega) \equiv \chi_{jj}(i\omega_\ell \to \hbar\omega + i0)$.

The non-conservation of the current (i.e., finite $\dot{J}$) arises from the scattering by the wall. In fact eq. (8) and (12) lead to

$$\dot{J}_z \equiv \frac{i}{\hbar}[H, J_z] = i\left(\frac{e}{m}\right)\Delta \sum_{\mathbf{k}q\sigma} \sigma A_q a^\dagger_{\mathbf{k}+q}\sigma_x a_{\mathbf{k}}. \tag{31}$$

The imaginary-time correlation function is then calculated as

$$\chi_{jj}(i\omega_\ell) = -\frac{\hbar}{L}\left(\frac{e\Delta}{m}\right)^2 \sum_{kq\sigma} |A_q|^2 \frac{1}{\beta}\sum_n G_{k+q,n+\ell,-\sigma} G_{kn\sigma}. \tag{32}$$

The summation over ω_n is carried out to obtain

$$\chi_{jj}(i\omega_\ell) = -\frac{\hbar}{L}\left(\frac{e\Delta}{m}\right)^2 \sum_{kq\sigma} |A_q|^2 \frac{f(\epsilon_{k+q,-\sigma}) - f(\epsilon_{k,\sigma})}{\epsilon_{k+q,-\sigma} - \epsilon_{k,\sigma} - i\omega_\ell}, \tag{33}$$

Thus the resistivity is calculated as

$$\begin{aligned}
\rho_{\rm c} &= \frac{\pi\Delta^2}{e^2 n^2}\frac{1}{V}\sum_{\mathbf{k}q\sigma} |A_q|^2 \delta(\epsilon_{\mathbf{k}+q,-\sigma} - \epsilon_{\mathbf{k},\sigma})\delta(\epsilon_{\mathbf{k},\sigma}) \\
&\simeq \frac{\pi^2\Delta^2}{2e^2 n^2 V} n_{\rm w} \sum_\sigma N_\sigma \int_{-\infty}^{\infty} \frac{dq}{\cosh^2 \frac{\pi}{2} q\lambda} \int_{-1}^{1} \frac{d\cos\theta}{2} \delta\left(\frac{\hbar k_{F\sigma} q}{m}\cos\theta + 2\sigma\Delta\right) \\
&= \frac{m^2\Delta^2}{4e^2 n^2 \hbar^3} n_{\rm w} \sum_\sigma \int_{\Lambda_{\rm c}(\sigma)}^{\infty} \frac{dx}{x}\frac{1}{\cosh^2 x},
\end{aligned} \tag{34}$$

where $\Lambda_c(\sigma) \equiv (\pi m\Delta\lambda/k_{F\sigma}\hbar^2)$ and $x \equiv \pi q\lambda/2$. In bulk ferromagnet with thick wall ($\lambda \gg k_F^{-1}$) and not very small Zeeman splitting, Λ_σ is large and thus the resistivity due to the wall is exponentially small,

$$\rho_{\rm c} \simeq \frac{m^2\Delta^2 n_{\rm w}}{2e^2 n^2\hbar^3}\sum_\sigma \frac{e^{-2\Lambda_\sigma}}{\Lambda_\sigma} \qquad (\tau \to \infty, \Lambda_\sigma \gg 1). \tag{35}$$

This is because the electron spin can follow adiabatically the rotation of the magnetization as it passes through the wall and so there will be very small reflection [19].

On the other hand in nanoscale contacts where the thickness of the wall can be determined mostly by the sample geometry, the wall can be very thin [27]. In this limit, $\lambda_c \to 0$, we obtain

$$\rho_{\rm c} \simeq \frac{m^2\Delta^2 n_{\rm w}}{4e^2 n^2\hbar^3}\sum_\sigma |\ln\Lambda_\sigma| \qquad (\tau \to \infty, \Lambda_\sigma \to 0). \tag{36}$$

Thus the resistance due to the wall, $R_{\rm c} \equiv \rho_{\rm c} L/A_\perp$ in this case is obtained as

$$R_{\rm c} = \frac{h}{e^2}\frac{9\pi^3}{32}\frac{(k_{F+}^2 - k_{F-}^2)^2}{(k_{F+}^3 + k_{F-}^3)^2 A_\perp}\left|\ln\left(\frac{\pi}{4}\right)^2 \frac{(k_{F+}^2 - k_{F-}^2)^2\lambda^2}{k_{F+}k_{F-}}\right|. \tag{37}$$

It is seen that in the case of atomic size contact the resistance due to a domain wall can be of order of h/e^2, and thus a large magnetoresistance is expected by switching the magnetization direction in a atomic size contact, where the conductance in the absence of the wall is of order of quantized conductance, e^2/h [27]. In contrast in disordered case the effect in the limit of thin wall is not as large as in the ballistic case [27].

It is interesting that the result of the resistivity based on Kubo formula, eq. (26) with $\sigma_{\rm c}$ given by (25), has the identical limiting value at $\tau \to \infty$ (the first term in eq. (D9)) as the result of Mori formula (eq. (34)), which suggests that the Kubo formula calculation remains correct in this limit, although the perturbative treatment used there becomes invalid. Furthermore it turns out that if we assume finite lifetime for the electron in Mori formula,

which is again without justification, the result is identical to the result of Kubo formula (26). In fact Mori formula treated this way leads to

$$\rho_{\rm c} = (en)^{-2}\,\frac{\hbar^3}{4\pi}\left(\frac{\hbar\Delta}{\tau}\right)^2\frac{1}{V}\sum_{\mathbf{k}q\sigma}|A_q|^2\frac{1}{\left[\epsilon^2_{\mathbf{k}-\frac{q}{2},\sigma}+\left(\frac{\hbar}{2\tau}\right)^2\right]\left[\epsilon^2_{\mathbf{k}+\frac{q}{2},-\sigma}+\left(\frac{\hbar}{2\tau}\right)^2\right]}, \tag{38}$$

and this is shown to be equivallent to eqs. (25) and (26) by similar calculation as in §D. These facts may indicate the correctness of the expression (25) and (26) for any value of τ.

III. QUANTUM CORRECTION

In the clean case, where $k_F\ell$ is large, the classical theory of transport considered in the previous section describes the electronic resistivity well. In disordered case with smaller $k_F\ell$, a correction becomes necessary, since the quantum nature of the electron begins to be important as a result of strong scattering by elastic impurities. Elastic impurities are those which cause only elastic scattering and thus do not destroy the coherence of the electron. In this case the scattered electron wave interferes with the incoming wave, and a state like a standing wave is formed. In this weakly localized state the conductivity is suppressed due to the quantum interference. The effect is stronger in lower dimensions, where the backward scattering occurs more effectively. This weakly localized state is described conveniently in terms of an amplitude of two electrons propagating in opposite direction interacting with each other through multiple impurity scatterings (Fig. 4). This process of particle-particle propagation is called Cooperon. The amplitude is related to the amplitude of the backward scattering, and is shown to grow at long wavelength because of the quantum interference. In fact Cooperon for the two incoming electrons with the same spin σ and the momentum of k_F and $-k_F+q$ is calculated at small q and small thermal frequencies (ω_n and $\omega_{n'}$) as [33]

$$\Gamma^{\sigma\sigma}_{+-}(q) \simeq \frac{n_{\rm i}v^2}{(Dq^2+\omega_n-\omega_{n'})\tau} \equiv \Gamma_0(q, n-n'), \tag{39}$$

where $D \equiv (\hbar^2k_F^2\tau/3m^2)$ and $_{+-}$ denotes $\omega_n > 0$ and $\omega_{n'} < 0$ (See Appendix E). (In calculating the quantum correction in this section we neglect difference between two $k_{F\sigma}$'s, i.e., quantity of $O(\Delta/\epsilon_F)$ for simplicity.) We consider here a ferromagnet with $\Delta\tau/\hbar \gg 1$ and then Cooperons connecting the electrons with opposite spin does not lead to any singular contribution and is thus neglected (Appendix E).

In (39) we have neglected the effect of inelastic scattering. In reality, the singularity of eq. (39) is smeared out due to the inelastic scattering (e.g., by phonons, electron-electron interaction and spin flip scattering by magnetic impurities) at finite temperature. Here we treat these inelastic scattering phenomenologically by introducing an inelastic lifetime, τ_φ (see Refs. [32,33] for microscopic discussion). A finite value of τ_φ indicates that the coherence is kept only to the spatial scale of $\ell_\varphi \equiv \sqrt{D\tau_\varphi}$. The Cooperon is modified then to be

$$\Gamma_0(q, n-n') = \frac{n_{\rm i}v^2}{(Dq^2+\omega_n-\omega_{n'}+1/\tau_\varphi)\tau}. \tag{40}$$

In the calculation of the static conductivity the thermal frequencies in the Cooperon (ω_n and $\omega_{n'}$) can be set equal to zero, and thus we write $\Gamma_0(q) \equiv \Gamma_0(q, \omega_n = 0)$ in this section. In terms of the Cooperon the quantum correction to the conductivity is written in the absence of the wall as (eq. (E9))

$$\sigma_{0\rm q} = -\frac{1}{2\pi}\left(\frac{e\hbar}{m}\right)^2\frac{1}{V}\frac{4\pi\hbar k_F^2}{3}N(0)\left(\frac{\tau}{\hbar}\right)^3\sum_{\mathbf{q},\sigma}\Gamma_0(q), \tag{41}$$

which is diagramatically expressed as in Fig. 5. This diagram is called a maximally crossed diagram, since the lines denoting the impurity scattering is crossing each other maximally. The quantum correction is rewritten as

$$\begin{aligned}\sigma_{0\rm q} &\simeq -2\sigma_0\left(\frac{\tau}{\hbar}\right)^2\sum_{\mathbf{q}}\Gamma_0(q)\\ &= -2\pi\sigma_0\left(\frac{\tau}{\hbar}\right)\frac{\hbar^2}{mk_F}\frac{1}{V}\sum_{\mathbf{q}}\frac{1}{Dq^2\tau+\kappa_\varphi},\end{aligned} \tag{42}$$

where $\kappa_\varphi \equiv \tau/\tau_\varphi$ and we have used $2\pi n_{\rm i} v^2 N(0)\tau/\hbar = 1$. The summation over q is cut off for small q at $q_z \sim \pi L^{-1}$ in the wire direction and $q_\perp \sim \pi L_\perp^{-1}$ in the perpendicular direction. Here we consider the case where the perpendicular dimension of the wire is small as compared with inelastic diffusion length, namely $L_\perp \lesssim \ell_\varphi$. In this case q-summation can be carried out in one-dimension along z-direction and we obtain

$$\frac{1}{V}\sum_{\mathbf{q}} \frac{1}{Dq^2\tau + \kappa_\varphi} = \frac{1}{L_\perp^2}\frac{1}{\pi}\int_{\pi/L}^{\pi/\ell} dq \frac{1}{(q\ell)^2/3 + \kappa} \simeq \frac{3\ell_\varphi}{2L_\perp^2\ell^2}, \tag{43}$$

where we have used $\kappa \ll 1$. In the last equality we used $L \gg \ell_\varphi$, which we assume. The result of the conductivity correction is thus

$$\sigma_{0\rm q} \simeq -3\pi\sigma_0 \frac{\ell_\varphi}{k_F^2 \ell L_\perp^2}. \tag{44}$$

A. Dephasing effect due to domain wall

Now we calculated the effect of the domain wall on the quantum correction. The quantum correction arises when the coherence of the electron system is modified by the wall. There is thus no effect if the magnetization change inside the wall is slow enough, in which case the electron can follow the magnetization change easily. The decoherence occurs due to a non-adiabatic process. In fact the first term in the interaction with the wall, eq. (8), can cause dephasing since it flips the electron spin. Thus the interference effect among electrons is suppressed due to this interaction with the wall. This dephasing effect is most conveniently studied in terms of the correction to the Cooperon. The correction to the Cooperon by the wall is shown up to the second order in Fig. 6. The process (a) is the most dominant contribution. Diagram (b) contributes to dephasing but is not important since it contains only one Cooperon and thus gives smaller contribution compared to process (a). Similar diagram (c) and the vertex correction type (d)(e) are neglected because they include Cooperons with different spins and thus are suppressed by a factor of $O(\hbar/\Delta\tau)$. The effect of dephasing due to the process (a) becomes clear by summing up higher order processes shown in Fig. 7, which gives rise to a mass of Cooperon (see eq. (52)). The Cooperon in the presence of the wall is calculated from these consideration as

$$\Gamma_{\rm w} \equiv \Gamma_0 + \Gamma_0^2 I_{\rm w} + \Gamma_0^3 I_{\rm w}^2 \cdots \simeq \Gamma_0 \left[\frac{1}{1 - \Gamma_0 I_{\rm w}}\right], \tag{45}$$

where

$$I_{\rm w} \equiv \sum_{\mathbf{k}'} (G_{\mathbf{k}',n,\sigma})^2 G_{-\mathbf{k}'+\mathbf{q},n',\sigma} \Sigma^{\rm w}_{\mathbf{k}',n,\sigma} + \text{c.c.}, \tag{46}$$

and

$$\Sigma^{\rm w}_{\mathbf{k}',n,\sigma} \equiv \left(\frac{\hbar^2}{2m}\right)^2 \sum_{q//z} \left(k_z' + \frac{q}{2}\right)^2 |A_q|^2 G_{\mathbf{k}'+q,n,-\sigma}, \tag{47}$$

is the self-energy due to the wall scattering. For the case of $k_F\lambda \gg 1$ and $\Delta\tau/\hbar \gg 1$ we are considering, this is evaluated in the case of electron at the Fermi energy ($|\mathbf{k}'| = k_F$) as (we consider the case $\omega_n > 0$)

$$\begin{aligned}
\Sigma^{\rm w}_{\mathbf{k}',n,\sigma} &= \left(\frac{\hbar^2}{2m}\right)^2 \frac{1}{\frac{i\hbar}{2\tau} - \epsilon_{\mathbf{k}'+q,-\sigma}} \sum_{q//z} \left(k_F\cos\theta + \frac{q}{2}\right)^2 |A_q|^2 \\
&\simeq \left(\frac{\hbar^2 k_F\cos\theta}{2m}\right)^2 \frac{1}{\frac{i\hbar}{2\tau} - 2\sigma\Delta} \sum_{q//z} |A_q|^2 \\
&= 2\left(\frac{\hbar^2 k_F\cos\theta}{2m}\right)^2 \frac{1}{\frac{i\hbar}{2\tau} - 2\sigma\Delta} \frac{n_{\rm w}}{\lambda},
\end{aligned} \tag{48}$$

where θ is the angle of the incoming momentum $\mathbf{k}'$ measured from the z-axis.

Its imaginary part of $\Sigma^{\rm w}$ is related to the life-time due to the scattering by the wall as

$$\frac{1}{\tau_{\rm w}(\theta,\sigma)} \equiv -\frac{2}{\hbar}{\rm Im}\Sigma^{\rm w}_{\mathbf{k}',n>0,\sigma} = \frac{1}{2}\frac{n_{\rm w}}{k_F^2\lambda}\left(\frac{\epsilon_F\cos\theta}{\Delta}\right)^2\frac{1}{\tau}. \tag{49}$$

The real part is neglected since it has only irrelevant effect of shifting the energy. By use of $\tau_{\rm w}$, $I_{\rm w}$ of (46) is calculated as

$$I_{\rm w} \simeq -\frac{i}{2}N(0)\int_{-\infty}^{\infty}d\epsilon\frac{1}{\left(\frac{i\hbar}{2\tau}-\epsilon\right)^2\left(-\frac{i\hbar}{2\tau}-\epsilon\right)}\left\langle\frac{1}{\tau_{\rm w}(\theta)}\right\rangle + {\rm c.c.} = -2\pi N(0)\kappa_{\rm w}, \tag{50}$$

where brackets denotes the average over θ and $\kappa_{\rm w}$ is given as

$$\kappa_{\rm w} \equiv \left\langle\frac{\tau}{\tau_{\rm w}}\right\rangle = \frac{n_{\rm w}}{6\lambda k_F^2}\left(\frac{\epsilon_F}{\Delta}\right)^2. \tag{51}$$

We therefore obtain the Cooperon in the presence of the wall (eq. (45)) as

$$\Gamma_{\rm w}(\mathbf{q}) = \frac{n_{\rm i}v^2}{Dq^2\tau+\kappa_\varphi+\kappa_{\rm w}}. \tag{52}$$

It is seen that the spin flip scattering by the wall contributed to an additional dephasing time. Note that the electron in the Cooperon here refers to the electron after the gauge transformation (5) , i.e., a.

In the presence of the wall, the quantum corrections given by eq. (42)) but with Γ_0 replaced by $\Gamma_{\rm w}$. Thus the contribution of the wall to the quantum correction is given by (by use of (42))

$$\delta\sigma_{\rm q} = 2\sigma_0\left(\frac{\tau}{\hbar}\right)^2\sum_{\mathbf{q}}(\Gamma_0(q)-\Gamma_{\rm w}). \tag{53}$$

In the same way as eq. (44), we obtain

$$\delta\sigma_{\rm q} = \sigma_0\frac{\sqrt{3}\pi}{k_F^2L_\perp^2}\left(\frac{1}{\sqrt{\kappa_\varphi}}-\frac{1}{\sqrt{\kappa_\varphi+\kappa_{\rm w}}}\right). \tag{54}$$

This quantum correction is positive, since the wall suppresses the localization by causing the dephasing.

IV. TOTAL RESISTIVITY DUE TO DOMAIN WALL

We have calculated both the classical and quantum contribution to the conductivity from the wall. The full conductivity due to the wall is obtained as $\Delta\sigma_{\rm w} \equiv \sigma_{\rm c}+\delta\sigma_{\rm q}$ from eqs. (25) and (54). In the clean limit there is no quantum correction. In the case of the disordered case with conditions (27) and (28) satisfied, the full correction to the conductivity by the wall is obtained as (by use of $\sigma_0 = \frac{e^2}{\hbar}\frac{k_F^2\ell}{3\pi^2}$)

$$\Delta\sigma_{\rm w} = \sigma_0\left[-\frac{3}{2}\frac{n_{\rm w}}{k_F^2\lambda}+\frac{\sqrt{3}\pi}{(k_FL_\perp)^2}\left(\frac{1}{\sqrt{\kappa_\varphi}}-\frac{1}{\sqrt{\kappa_\varphi+\kappa_{\rm w}}}\right)\right], \tag{55}$$

where we have neglected $o(\Delta/\epsilon_F)$. The conductivity in the absence of the wall is expressed including the quantum correction ($\sigma_{0{\rm q}}$) as

$$\sigma = \sigma_0\left[1-\frac{\sqrt{3}\pi}{(k_FL_\perp)^2}\frac{1}{\sqrt{\kappa_\varphi}}\right]. \tag{56}$$

In terms of the resistivity, which is the reciprocal of the conductivity, the wall contribution is obtained as $\Delta\rho_{\rm w} \equiv (\sigma + \Delta\sigma_{\rm w})^{-1} - \sigma^{-1} \simeq -\Delta\sigma_{\rm w}/\sigma^2$. The relative ratio of the wall contribution and the full resistivity ($\rho \equiv \sigma^{-1}$) is thus obtained as

$$\frac{\Delta\rho_{\rm w}}{\rho} \simeq \frac{3}{2}\frac{n_{\rm w}}{k_F^2\lambda} - \frac{\sqrt{3}\pi}{(k_F L_\perp)^2}\left(\frac{1}{\sqrt{\kappa_\varphi}} - \frac{1}{\sqrt{\kappa_\varphi + \kappa_{\rm w}}}\right), \tag{57}$$

where we have neglected the quantum correction in ρ^{-1} (eq. (56)). The first term is the classical contribution and the second term is the quantum contribution, which reduces the resistivity. The classical contributions $n_{\rm w}/(k_F^2\lambda)$ is proportional to the reflection probability caused by the interaction (8), which is not large in conventional $3d$ transition metals where $k_F\lambda$ is large. The quantum contribution is also proportional to this probability (it is essentially $\tau_{\rm w}^{-1}$ of eq. (51)), but in this case the effect is enhanced at by the coherence, as indicated by a large factor of $1/\sqrt{\kappa_\varphi}$. Thus at lower temperature where κ_φ is smaller the quantum dephasing effect wins over the classical effect and thus the resistivity contribution from the wall can be negative (see below).

In experiments the effect of dephasing by the wall would be separated from other classical effects by looking into the temperature dependence. In fact the dephasing due to phonons, electron-electron interaction is known to decrease at lower temperature, typically by a power law, $\tau_\varphi^{-1} \propto T^\alpha$, α being a constant of $O(1)$ [32,33]. Thus according to the result (57) the decrease of the resistivity due to the dephasing effect will increase as

$$\frac{\Delta\rho_{\rm w}}{\rho} \propto T^{-3\alpha/2}, \tag{58}$$

in the region $\tau_{\rm w}^{-1} \ll \tau_\varphi^{-1}$.

It has been discussed that at low temperature, e.g. below 1K, the dephasing time τ_φ is mostly due to the electron-electron interaction [32,33]. The temperature dependence of τ_φ in this case has been estimated to be $\tau_\varphi^{-1} \simeq [(k_B T/\sqrt{\tau})/(k_F L_\perp)^2]^{2/3}$ in wires, and thus $\alpha = 2/3$ [67]. Let us consider a wire of $L_\perp = 150$Å ($K_F L_\perp = 100$, $k_F^{-1} \simeq 1.5$Å). If the elastic mean free path is $\ell \sim 30$Å, which corresponds to $\epsilon_F\tau/\hbar \sim 10$, the above expression leads to $\kappa_\varphi = \tau/\tau_\varphi \simeq 0.22 \times 10^{-4}$ at $T = 1$K. The dephasing effect due to the wall is calculated from eq. (51). Considering a wire length of $L = n_{\rm w}^{-1} = 1000$Å and a thin wall $k_F\lambda = 200$ as observed in Co film [18] and choosing $\Delta/\epsilon = 0.2$, we obtain $\kappa_{\rm w} = 3.1 \times 10^{-5}$. The relative contribution from the wall $\Delta\rho_{\rm w}/\rho$ in this case is then calculated as $\Delta\rho_{\rm w}/\rho = -0.051$. Note that the classical contribution in this case is smaller than the quantum contribution by a factor of 10^{-4}. This decrease of resistivity would be large enough to observe in experiments.

A. Effect of internal field on coherence

In ferromagnets the total magnetic field is given by $B = H + 4\pi M$, where H is the external field and $4\pi M$ is an internal magnetic field due to the magnetization. In the case of clean Fe wire ($\ell \sim 1.4\mu$m) the internal field $4\pi M$ is estimated from the of the behavior of the magnetoresistance due to the Lorentz motion (at external magnetic field of about 0.1T) as $4\pi M \simeq 2.2$T [5]. This large magnetic field can destroy the coherence and thus weak localization in the case of film or bulk sample [32,33]. In contrast in mesoscopic wires the effect can be neglected if the wire is narrow enough. In fact, in the case of magnetization along the wire direction, the magnetic flux penetrating though the wire is $\Phi = 4\pi M L_\perp^2$. The modification of the interference of the electron becomes important if this flux is comparable to the unit flux $\Phi_0 \equiv h/2e = 2.1 \times 10^{-15}$[Tm^2]. Thus if $L_\perp \lesssim 300$Å, the magnetic flux contained in any electron path is too small to affect the coherence.

The effect of Lorentz motion dut to this internal field is neglected in disordered case since the parameter which determines the effect, $\omega_c\tau$ ($\omega_c \equiv eB/m$), is small (for $B = 2.2T$ and $\ell = 30$Å, $\omega_c\tau \simeq 10^{-3}$).

V. CONDUCTANCE FLUCTUATION DUE THE WALL MOTION

So far we have studied the resistivity due to a static wall. In this section we will discuss the change of the electron transport due to the motion of the wall. Here we will discuss the conductance of the sample, $G \equiv \sigma \times (A_\perp/L)$, $A_\perp$ being the crosssectional area of the wire. The wall motion can affect the conductance in several different manner, but the most significant effect will be that due to the quantum interference. It has been shown in disordered metal that the fluctuation of the conductance can arise at low temperature as a consequence of quantum interference and that such fluctuation is of universal order of $e^2/h = 3.9 \times 10^{-5}\Omega^{-1}$ independent of sample size and dimensions [68]. It

has been shown further that if a single impurity atom changes its position in such cases, the interference pattern can change and as a result the conductance of the entire system can change by $O(e^2/h)$ [35]. Thus we may expect similar effect of conductance change to arise due to the motion of domain walls. Within the argument of classical resistivity, no change of Boltzmann resistivity is expected since it is determined by the reflection probability by the wall, which does not depend on the wall position. If we take into account the quantum interference among the electron, however, the motion can affect the conductance change by changing the interference pattern.

In the experimental situations, the conductance change of a classical origin would also be possible, since the wall motion means the change of the total magnetization, and this, according to the argument of the anisotropic magnetoresistance [3], can lead to the resistivity change. In this case the expected change for the motion of the wall over a distance of $r(\ll L)$ is $\delta\rho \simeq \Delta\rho_{\rm ani} \times (r/L)$, $\Delta\rho_{\rm ani}$ being the magnitude of anisotropic magnetoresistance; $\Delta\rho_{\rm ani} \equiv {\rm Max}(\rho(H)) - {\rm Min}(\rho(H))$. In fact this is what is claimed by Hong and Giordano [9] to be the origin of the observed jump in resistivity of Ni wire. Compared to this classical conductance change, that of a quantum origin is much more sensitive to a small motion of a wall. Actually it turns out that a displacement of a wall over 100Å can give rise to a conductance change sufficiently large to be observed.

If we write the conductance of the sample with a domain wall at $z = r$ as $G(r)$, we are interested in the difference $\delta G \equiv G(r) - G(0)$. Within the formulation based on Kubo formula, however, we cannot directly calculate the conductance G or its change δG of a fixed sample, since we do not know the particular configuration of impurities of the sample. We can only calculate the conductance averaged over the impurity configurations, in other words, over many samples (this is not so of course in numerical calculations). Thus we will estimate the mean square of difference of the conductance

$$< (\delta G)^2 >_{\rm imp} = 2[< G(0)^2 >_{\rm imp} - < G(r)G(0) >_{\rm imp}], \tag{59}$$

where $<>_{\rm imp}$ denotes the average over impurity configurations. The quantity $< G(r)G(0) >_{\rm imp}$ is expressed as

$$< G(r)G(0) >_{\rm imp} = \left(\frac{A_\perp}{L}\right)^2 \lim_{\omega,\omega'\to 0} \frac{1}{\omega\omega'}[F(r, i\omega_\ell = \omega + i0, i\omega_{\ell'} = \omega' + i0) - F(r, 0 + i0, 0 + i0)], \tag{60}$$

where

$$F(r, i\omega_\ell, i\omega_{\ell'}) \equiv \frac{\hbar^2}{V^2} < [J(i\omega_\ell)J(-i\omega_\ell)]_{z=r}[J(i\omega_{\ell'})J(-i\omega_{\ell'})]_{z=0} > . \tag{61}$$

This correlation function is represented diagramatically by two electron loops connected through the interaction with the domain wall. Diagrams with two loops which are not connected by the domain wall line does not contribute to $< (\delta G)^2 >_{\rm imp}$ because this quantity is a difference of the cases with $z = r$ and $z = 0$. The simplest contribution to $< G(r)G(0) >_{\rm imp}$ at the lowest, i.e., fourth, order in domain walls is that shown in Fig. 8(a) and (a'). The domain wall is at $z = r$ in the outer loop and is at $z = 0$ in the inner loop. Four Cooperons are included in these processes. To calculate the contribution (a), let us first look into the part shown in Fig. 9. The domain wall line here is associated with a factor of e^{-ipr}, since one of the electron line here interacts with the wall at $z = r$ and the other with $z = 0$. Important contribution comes from the two cases of $n' > 0, n < 0$ and $n' < 0, n > 0$, in which case the amplitude $\delta\Gamma_{\rm w}$ is written as

$$\begin{aligned}\delta\Gamma_{\rm w}(\mathbf{q}, n' - n) = \left(\frac{\hbar^2}{2m}\right)^2 (\Gamma_0(\mathbf{q}, n' - n))^2 \sum_{\mathbf{k},p,\sigma} \left(k_z + \frac{p}{2}\right)\left(-k_z + q_z - \frac{p}{2}\right)|A_p|^2 e^{-ipr} \\ \times G_{\mathbf{k},n,\sigma} G_{\mathbf{k}+p,n,-\sigma} G_{-\mathbf{k}+\mathbf{q},n',\sigma} G_{-\mathbf{k}+\mathbf{q}-p,n',-\sigma},\end{aligned} \tag{62}$$

where Cooperons Γ_0 is defined in eq.(39). This is evaluated in the case of $q, p \ll k_F$ and the result neglecting quantities of $O(\Delta/\epsilon_F)^2$ is

$$\delta\Gamma_{\rm w} \simeq -\left(\frac{\hbar^2}{2m}\right)^2 \frac{\pi N(0) k_F^2 \tau}{3\hbar\Delta^2} \Gamma_0^2 \sum_p |A_p|^2 e^{-ipr}. \tag{63}$$

The p-summation here results in

$$\begin{aligned}\sum |A_p|^2 e^{-ipr} &= \frac{2n_{\rm w}}{\lambda} \frac{r/\lambda}{\sinh(r/\lambda)} \\ &= \frac{2n_{\rm w}}{\lambda} W\left(r/\lambda\right),\end{aligned} \tag{64}$$

where

$$W(x) \equiv \frac{x}{\sinh x}. \tag{65}$$

We thus obtain

$$\delta\Gamma_{\rm w}(\mathbf{q}, n'-n) \simeq -2\kappa_{\rm w}\frac{n_{\rm i}v^2}{\tau^2}(\tilde{\Gamma}_0(q,n'-n))^2 W(r/\lambda), \tag{66}$$

where

$$\tilde{\Gamma}_0(q,n) \equiv \frac{\tau}{n_{\rm i}v^2}\Gamma_0(q,n) = \frac{1}{D\mathbf{q}^2+\omega_n}, \tag{67}$$

and $\kappa_{\rm w}$ is the dephasing time due to the wall defined in eq. (51). (we suppress here the inelastic lifetime.) By use of this $\delta\Gamma$, the process of Fig. 8(a) is written as (4 in the suffix denotes four Cooperons)

$$\begin{aligned} F_{4\rm a}(\omega_\ell,\omega_{\ell'}) &= \left(\frac{e\hbar}{m}\right)^4 \frac{1}{V^2}\sum_{\mathbf{k},\mathbf{k}',\mathbf{q},\sigma}\frac{1}{\beta^2}\sum_{n,n'} k_z(-k+q)_z k'_z(-k'+q)_z \\ &\quad\times G_{\mathbf{k},n+\ell,\sigma}G_{\mathbf{k},n,\sigma}G_{-\mathbf{k}+\mathbf{q},n'+\ell',\sigma}G_{-\mathbf{k}+\mathbf{q},n',\sigma}G_{\mathbf{k}',n+\ell,-\sigma}G_{\mathbf{k}',n,-\sigma}G_{-\mathbf{k}'+\mathbf{q},n'+\ell',-\sigma}G_{-\mathbf{k}'+\mathbf{q},n',-\sigma} \\ &\quad\times\delta\Gamma_{\rm w}(q,|n+\ell-n'|)\delta\Gamma_{\rm w}(q,|n-(n'+\ell')|) \\ &\simeq F_0\frac{W(r/\lambda)^2}{\tau^4}\frac{1}{\beta^2}{\sum_{n,n'}}'(\tilde{\Gamma}_0(q,|n+l-n'|))^2(\tilde{\Gamma}_0(q,|n-(n'+\ell')|))^2, \end{aligned} \tag{68}$$

where

$$F_0 \equiv \left[\left(\frac{e\hbar}{m}\right)^2\frac{4k_F^2}{3V}\kappa_{\rm w}\tau^2\right]^2. \tag{69}$$

The summation over the Matsubara frequencies, $\sum'_{n,n'}$, is restricted to the following three cases where the Cooperons has a singular contributions (ℓ and ℓ' are positive);

$$\begin{array}{lll} \text{I}: & n+\ell, n>0, & n'+\ell', n'<0 \\ \text{II}: & n+\ell, n<0, & n'+\ell', n'>0 \\ \text{III}: & n+\ell, n'+\ell'>0, & n, n'<0. \end{array} \tag{70}$$

Adding the contributions from these three cases and taking the terms linear in both ω_ℓ and $\omega_{\ell'}$, which are relevant to the conductance change, we obtain (see Appendix F)

$$\frac{F_{4\rm a}}{\omega_\ell\omega_{\ell'}} \simeq \frac{F_0W^2}{\tau^4}[12J_6+J'_6], \tag{71}$$

where

$$J_m \equiv \frac{1}{\beta^2}\sum_{n,n'=0}^{\infty}\frac{1}{(D\mathbf{q}^2+\omega_n+\omega_{n'})^m}, \tag{72}$$

and

$$\begin{aligned} J'_6 \equiv \frac{1}{\beta^2}\sum_{n,n'=0}^{\infty}\Bigg[&-8\frac{1}{(D\mathbf{q}^2+\omega_n+\omega_{n'})^3(D\mathbf{q}^2-(\omega_n+\omega_{n'}))^3} \\ &+6\left\{\frac{1}{(D\mathbf{q}^2+\omega_n+\omega_{n'})^2(D\mathbf{q}^2-(\omega_n+\omega_{n'}))^4}\right. \\ &\left.+\frac{1}{(D\mathbf{q}^2+\omega_n+\omega_{n'})^4(D\mathbf{q}^2-(\omega_n+\omega_{n'}))^2}\right\}\Bigg]. \end{aligned} \tag{73}$$

It can be shown by similar calculation that the process Fig. 8(a') leads to a different factor in front of J_6;

$$\frac{F_{4a'}}{\omega_\ell\omega_{\ell'}} \simeq \frac{F_0W^2}{\tau^4}8J_6. \tag{74}$$

Hence the contributions from the four Cooperons, $F_4 \equiv F_{4a} + F_{4a'}$, is obtained as

$$\frac{F_4}{\omega_\ell\omega_{\ell'}} \simeq \frac{F_0W^2}{\tau^4}[20J_6 + J_6']. \tag{75}$$

Processes with five Cooperons are shown in Fig. 10. Although they contains two more Cooperons, the contributions turns out to be the same order as four Cooperons processes. The result of these processes are (Appendix G)

$$\frac{F_5}{\omega_\ell\omega_{\ell'}} = -720F_0W\left(r/\lambda\right)^2\frac{Dq_z^2}{\tau^4}J_7. \tag{76}$$

Similarly contributions from six Cooperons shown in Fig. 11 are calculated as (Appendix G)

$$\frac{F_6}{\omega_\ell\omega_{\ell'}} = 3024F_0W\left(r/\lambda\right)^2\frac{(Dq_z^2)^2}{\tau^4}J_8. \tag{77}$$

From these results the total correlation function $F \equiv F_4 + F_5 + F_6$ is given as

$$\frac{F(i\omega_\ell, i\omega_{\ell'})}{\omega_\ell\omega_{\ell'}} = \frac{F_0W^2}{\tau^4}\left[20J_6 + J_6' - 720Dq_z^2J_7 + 3024(Dq_z^2)^2J_8\right]. \tag{78}$$

By use of contour integration J_m's are calculated as (AppendixH)

$$J_m = \frac{1}{(2\pi)^2(m-1)(m-2)}\frac{1}{(Dq^2)^{m-2}}, \tag{79}$$

and similarly $J_6' = 1/[(2\pi)^2(Dq^2)^4]$. Thus

$$\frac{F(i\omega_\ell, i\omega_{\ell'})}{\omega_\ell\omega_{\ell'}} = \frac{F_0W^2}{(2\pi)^2\tau^4}\left[1 + 1 - 8 + \frac{72}{5}\right]\sum_q\frac{1}{(Dq^2)^4}. \tag{80}$$

The summation over q is carried out in one-dimension similarly to eq. (43). The result is (recovering τ_φ and $\tau_{\rm w}$ in Cooperons)

$$\begin{aligned}\frac{1}{\tau^4}\sum_q\frac{1}{(Dq^2 + 1/\tau_\varphi + 1/\tau_{\rm w})^4} &\simeq \frac{3^4L}{\pi\ell}\int_0^\infty\frac{dx}{(x^2+3\kappa)^4} \\ &= \frac{5\sqrt{3}}{32}\frac{L}{\ell}\frac{1}{\kappa^{7/2}},\end{aligned} \tag{81}$$

where $\kappa \equiv \kappa_\varphi + \kappa_{\rm w}$. The conductance change is obtained by used of this and eqs. (59)(60)(80) as

$$\delta G \simeq \frac{e^2}{\hbar}\kappa_{\rm w}\sqrt{1 - [W\left(r/\lambda\right)]^2}\sqrt{\frac{7}{2\sqrt{3}\pi^2}}\sqrt{\left(\frac{\ell}{L}\right)^3\frac{1}{\kappa^{7/2}}}. \tag{82}$$

VI. SUMMARY

We have studied the effect of the domain wall on electronic transport properties in wire of ferromagnetic metals. We considered the case of $3d$ transition metals, and took into account the scattering by impurities as well. We have first calculated the conductivity within the classical (Boltzmann) transport theory by use of linear response theory. This contribution turns out to be negligiblly small in bulk magnets, but it can be significant in ballistic nanocontacts, as indicated in recent experiments. Second we discussed the quantum correction of the conductivity due to the wall in the disordered case. This contribution is due to the dephasing effect caused by the wall and thus gives negative contribution to the resistivity. this effect grows at lower temperature and can win over the classical contribution, in particular in wire of diameter $L_\perp \lesssim \ell_\varphi$, ℓ_φ being the inelastic diffusion length.

So far the studies of transport in magnetic metals has been carried out mostly in the system of low resistivity and high temperature, partially because of the possible application to devices. Our main message here is that in disordered system magnetism can affect the transport properties in a novel way by changing the quantum coherence among electrons at low temperature. At present there are no experiment which clearly indicate this effect, but it will be observed in the near future, for instance, in narrower wire with a long inelastic diffusion length.

ACKNOWLEDGEMENTS

The author is indebted to H. Fukuyama for collaboration on the preceeding letter, on which this paper is based. The author thanks G. Bauer, A. Brataas and N. Garcia for collaborations and discussions and K. Kuboki, H. Kohno, Y. Otani, K. Takanashi for valuable discussions. This work is partially supported by a Grand-in-Aid for Scientific Research on the Priority Area "Nanoscale Magnetism and Transport" (No.10130219) and "Spin Controlled Semiconductor Nanostructures" (No.10138211) from the Ministry of Education, Science, Sports and Culture. The author also thanks The Murata Science Foundation and Alexander von Humboldt Stiftung for finantial support.

APPENDIX A: CALCULATION OF CLASSICAL CONDUCTIVITY BY KUBO FORMULA

Here let us give the details of derivation of eq. (18). Firstly by use of

$$k_z(G_{\mathbf{k},n,\sigma})^2 = \frac{m}{\hbar^2}\frac{\partial}{\partial k_z}G_{\mathbf{k},n,\sigma}, \tag{A1}$$

and partial integration with respect to k_z, the self-energy term Q_2 is written as

$$\begin{aligned} Q_2 &= -\frac{B}{4}\frac{1}{\beta}\sum_n \frac{1}{V}\sum_{\mathbf{k}q\sigma} k_z|A_q|^2\partial_{k_z}(G_{\mathbf{k},n,\sigma}G_{\mathbf{k},n+\ell,\sigma}) \\ &= \frac{B}{4}\frac{1}{\beta}\sum_n \frac{1}{V}\sum_{\mathbf{k}q\sigma} |A_q|^2 G_{\mathbf{k},n,\sigma}G_{\mathbf{k},n+\ell,\sigma}, \end{aligned} \tag{A2}$$

where $B \equiv ((e\hbar)^2/2m^2)$. The other self-energy contribution, Q_4, can be rewritten by use of the identity

$$G_{\mathbf{k},n,\sigma}G_{\mathbf{k},n+\ell,\sigma} = \frac{1}{i\left(\omega_\ell + \Delta_{n\ell}\right)}(G_{\mathbf{k},n,\sigma} - G_{\mathbf{k},n+\ell,\sigma}), \tag{A3}$$

where

$$\Delta_{n\ell} \equiv \frac{\hbar}{2\tau}(\mathrm{sgn}(n+\ell) - \mathrm{sgn}(n)), \tag{A4}$$

as

$$\begin{aligned} Q_4 &= -\frac{B\hbar^4}{2m^2}\frac{1}{\beta}\sum_n \frac{1}{V}\sum_{\mathbf{k}q\sigma} k_z^2\left(k_z - \frac{q}{2}\right)^2|A_q|^2\frac{1}{i\left(\omega_\ell + \Delta_{n\ell}\right)} \\ &\quad\times[(G_{\mathbf{k}-\frac{q}{2},n,\sigma} - G_{\mathbf{k}-\frac{q}{2},n+\ell,\sigma})(G_{\mathbf{k}-\frac{q}{2},n,\sigma}G_{\mathbf{k}+\frac{q}{2},n,-\sigma} + G_{\mathbf{k}-\frac{q}{2},n+\ell,\sigma}G_{\mathbf{k}+\frac{q}{2},n+\ell,-\sigma})] \\ &= -\frac{B\hbar^4}{2m^2}\frac{1}{\beta}\sum_n \frac{1}{V}\sum_{\mathbf{k}q\sigma} k_z^2\left(k_z - \frac{q}{2}\right)^2|A_q|^2\frac{1}{i\left(\omega_\ell + \Delta_{n\ell}\right)} \\ &\quad\times[-G_{\mathbf{k}-\frac{q}{2},n,\sigma}G_{\mathbf{k}-\frac{q}{2},n+\ell,\sigma}(G_{\mathbf{k}+\frac{q}{2},n,-\sigma} - G_{\mathbf{k}+\frac{q}{2},n+\ell,-\sigma}) \\ &\quad+(G_{\mathbf{k}-\frac{q}{2},n,\sigma})^2G_{\mathbf{k}+\frac{q}{2},n,-\sigma} - (G_{\mathbf{k}-\frac{q}{2},n+\ell,\sigma})^2G_{\mathbf{k}+\frac{q}{2},n+\ell,-\sigma}] \\ &\equiv Q_{4a} + Q_{4b}, \end{aligned} \tag{A5}$$

where

$$\begin{aligned} Q_{4a} &\equiv \frac{B\hbar^4}{2m^2}\frac{1}{\beta}\sum_n \frac{1}{V}\sum_{\mathbf{k}q\sigma} k_z^2\left(k_z - \frac{q}{2}\right)^2|A_q|^2 G_{\mathbf{k}-\frac{q}{2},n,\sigma}G_{\mathbf{k}-\frac{q}{2},n+\ell,\sigma}G_{\mathbf{k}+\frac{q}{2},n,-\sigma}G_{\mathbf{k}+\frac{q}{2},n+\ell,-\sigma}, \\ Q_{4b} &\equiv -\frac{B\hbar^4}{2m^2}\frac{1}{\beta}\sum_n \frac{1}{V}\sum_{\mathbf{k}q\sigma} k_z^2\left(k_z - \frac{q}{2}\right)^2|A_q|^2\frac{1}{i\left(\omega_\ell + \Delta_{n\ell}\right)} \\ &\quad\times\left[(G_{\mathbf{k}-\frac{q}{2},n,\sigma})^2G_{\mathbf{k}+\frac{q}{2},n,-\sigma} - (G_{\mathbf{k}-\frac{q}{2},n+\ell,\sigma})^2G_{\mathbf{k}+\frac{q}{2},n+\ell,-\sigma}\right]. \end{aligned} \tag{A6}$$

The sum of the terms $Q_{4a} + Q_5$ can then be simplified as

$$Q_{4a}+Q_5=\frac{B\hbar^4}{4m^2}\frac{1}{\beta}\sum_n\frac{1}{V}\sum_{\mathbf{k}q\sigma}(k_zq)^2|A_q|^2G_{\mathbf{k}-\frac{q}{2},n,\sigma}G_{\mathbf{k}-\frac{q}{2},n+\ell,\sigma}G_{\mathbf{k}+\frac{q}{2},n,-\sigma}G_{\mathbf{k}+\frac{q}{2},n+\ell,-\sigma}. \tag{A7}$$

This expression can be rewritten further by use of the identity

$$\left(\frac{\hbar^2k_zq}{m}+2\sigma\Delta\right)G_{\mathbf{k}+\frac{q}{2},n,-\sigma}G_{\mathbf{k}-\frac{q}{2},n,\sigma}=G_{\mathbf{k}+\frac{q}{2},n,-\sigma}-G_{\mathbf{k}-\frac{q}{2},n,\sigma}, \tag{A8}$$

and the expression (A2) for Q_2 as

$$\begin{aligned}Q_{4a}+Q_5=&\frac{B}{4m^2}\frac{1}{\beta}\sum_n\frac{1}{V}\sum_{\mathbf{k}q\sigma}|A_q|^2[(2m\Delta)^2G_{\mathbf{k}-\frac{q}{2},n,\sigma}G_{\mathbf{k}-\frac{q}{2},n+\ell,\sigma}G_{\mathbf{k}+\frac{q}{2},n,-\sigma}G_{\mathbf{k}+\frac{q}{2},n+\ell,-\sigma}\\&+2m^2\sigma\Delta\{G_{\mathbf{k}-\frac{q}{2},n,\sigma}G_{\mathbf{k}+\frac{q}{2},n,-\sigma}(G_{\mathbf{k}-\frac{q}{2},n+\ell,\sigma}-G_{\mathbf{k}+\frac{q}{2},n+\ell,-\sigma})\\&+G_{\mathbf{k}-\frac{q}{2},n+\ell,\sigma}G_{\mathbf{k}+\frac{q}{2},n+\ell,-\sigma}(G_{\mathbf{k}-\frac{q}{2},n,\sigma}-G_{\mathbf{k}+\frac{q}{2},n,-\sigma})\}\\&+m^2(G_{\mathbf{k}-\frac{q}{2},n,\sigma}-G_{\mathbf{k}+\frac{q}{2},n,-\sigma})(G_{\mathbf{k}-\frac{q}{2},n+\ell,\sigma}-G_{\mathbf{k}+\frac{q}{2},n+\ell,-\sigma})]\\=&Q_{\rm c}+Q_1+2Q_2+Q'_{45},\end{aligned} \tag{A9}$$

where

$$Q_{\rm c}\equiv B\Delta^2\frac{1}{\beta}\sum_n\frac{1}{V}\sum_{\mathbf{k}q\sigma}|A_q|^2G_{\mathbf{k}-\frac{q}{2},n,\sigma}G_{\mathbf{k}-\frac{q}{2},n+\ell,\sigma}G_{\mathbf{k}+\frac{q}{2},n,-\sigma}G_{\mathbf{k}+\frac{q}{2},n+\ell,-\sigma}, \tag{A10}$$

is the term which survives in the final expression, (18), and

$$Q'_{45}\equiv B\frac{1}{\beta}\sum_n\frac{1}{V}\sum_{\mathbf{k}q\sigma}\sigma\Delta|A_q|^2[G_{\mathbf{k}-\frac{q}{2},n,\sigma}G_{\mathbf{k}+\frac{q}{2},n,-\sigma}G_{\mathbf{k}-\frac{q}{2},n+\ell,\sigma}+G_{\mathbf{k}-\frac{q}{2},n+\ell,\sigma}G_{\mathbf{k}+\frac{q}{2},n+\ell,-\sigma}G_{\mathbf{k}-\frac{q}{2},n,\sigma}]. \tag{A11}$$

Similarly by use of identities (A3) and (A8), Q_{4b} of (A6) is rewritten as

$$\begin{aligned}Q_{4b}=&-\frac{B\hbar^2}{2m}\frac{1}{\beta}\sum_n\frac{1}{V}\sum_{\mathbf{k}q\sigma}k_z^2\left(k_z-\frac{q}{2}\right)|A_q|^2\frac{1}{i\left(\omega_\ell+\Delta_{n\ell}\right)}\\&\times\left[(\partial_{k_z}G_{\mathbf{k}-\frac{q}{2},n,\sigma})G_{\mathbf{k}+\frac{q}{2},n,-\sigma}-(\partial_{k_z}G_{\mathbf{k}-\frac{q}{2},n+\ell,\sigma})G_{\mathbf{k}+\frac{q}{2},n+\ell,-\sigma}\right]\\=&-\frac{B\hbar^2}{2m}\frac{1}{\beta}\sum_n\frac{1}{V}\sum_{\mathbf{k}q\sigma}k_z^2|A_q|^2\frac{1}{i\left(\omega_\ell+\Delta_{n\ell}\right)}\\&\times\frac{1}{2}\left[\left(k_z-\frac{q}{2}\right)\left[(\partial_{k_z}G_{\mathbf{k}-\frac{q}{2},n,\sigma})G_{\mathbf{k}+\frac{q}{2},n,-\sigma}-(\partial_{k_z}G_{\mathbf{k}-\frac{q}{2},n+\ell,\sigma})G_{\mathbf{k}+\frac{q}{2},n+\ell,-\sigma}\right]\right.\\&\left.+\left(k_z+\frac{q}{2}\right)\left[G_{\mathbf{k}-\frac{q}{2},n,\sigma}\partial_{k_z}G_{\mathbf{k}+\frac{q}{2},n,-\sigma}-G_{\mathbf{k}-\frac{q}{2},n+\ell,\sigma}\partial_{k_z}G_{\mathbf{k}+\frac{q}{2},n+\ell,-\sigma}\right]\right]\\=&-\frac{B\hbar^2}{4m}\frac{1}{\beta}\sum_n\frac{1}{V}\sum_{\mathbf{k}q\sigma}k_z^3|A_q|^2\frac{1}{i\left(\omega_\ell+\Delta_{n\ell}\right)}\\&\times\partial_{k_z}\left[G_{\mathbf{k}-\frac{q}{2},n,\sigma}G_{\mathbf{k}+\frac{q}{2},n,-\sigma}-G_{\mathbf{k}-\frac{q}{2},n+\ell,\sigma}G_{\mathbf{k}+\frac{q}{2},n+\ell,-\sigma}\right]\\&+\frac{B\hbar^4}{4m^2}\frac{1}{\beta}\sum_n\frac{1}{V}\sum_{\mathbf{k}q\sigma}k_z^2q\left(k_z-\frac{q}{2}\right)|A_q|^2\frac{1}{i\left(\omega_\ell+\Delta_{n\ell}\right)}\\&\times\left[(G_{\mathbf{k}-\frac{q}{2},n,\sigma})^2G_{\mathbf{k}+\frac{q}{2},n,-\sigma}-(G_{\mathbf{k}-\frac{q}{2},n+\ell,\sigma})^2G_{\mathbf{k}+\frac{q}{2},n+\ell,-\sigma}\right]\\\equiv&Q'_{4b}+Q''_{4b}.\end{aligned} \tag{A12}$$

The first term ($\equiv Q'_{4b}$) turns out by use of partial integration to be

$$\begin{aligned}Q'_{4b}=&\frac{3B\hbar^2}{4m}\frac{1}{\beta}\sum_n\frac{1}{V}\sum_{\mathbf{k}q\sigma}k_z^2|A_q|^2\frac{1}{i\left(\omega_\ell+\Delta_{n\ell}\right)}\left[G_{\mathbf{k}-\frac{q}{2},n,\sigma}G_{\mathbf{k}+\frac{q}{2},n,-\sigma}-G_{\mathbf{k}-\frac{q}{2},n+\ell,\sigma}G_{\mathbf{k}+\frac{q}{2},n+\ell,-\sigma}\right]\\=&-\frac{3}{4}Q_{3a},\end{aligned} \tag{A13}$$

where Q_{3a} is the term which appears in the expression of Q_3,

$$Q_{3a} \equiv -\frac{B\hbar^2}{m}\frac{1}{\beta}\sum_n \frac{1}{V}\sum_{\mathbf{k}q\sigma} k_z^2 |A_q|^2 [G_{\mathbf{k}-\frac{q}{2},n,\sigma} G_{\mathbf{k}-\frac{q}{2},n+\ell,\sigma} G_{\mathbf{k}+\frac{q}{2},n,-\sigma} + G_{\mathbf{k}-\frac{q}{2},n+\ell,\sigma} G_{\mathbf{k}+\frac{q}{2},n,-\sigma} G_{\mathbf{k}+\frac{q}{2},n+\ell,-\sigma}]. \tag{A14}$$

The second term in (A12) is rewritten by use of (A8) and partial integration as $Q''_{4b} = Q_2 - (1/4)Q_{3a} + Q'_{\rm c}$ where

$$Q'_{\rm c} \equiv -\frac{B}{2}\frac{1}{\beta}\sum_n \frac{1}{V}\sum_{\mathbf{k}q\sigma} \sigma \Delta k_z |A_q|^2 \frac{1}{i\left(\omega_\ell + \Delta_{n\ell}\right)} \left[G_{\mathbf{k}+\frac{q}{2},n,-\sigma}\partial_{k_z} G_{\mathbf{k}-\frac{q}{2},n,\sigma} - G_{\mathbf{k}+\frac{q}{2},n+\ell,-\sigma}\partial_{k_z} G_{\mathbf{k}-\frac{q}{2},n+\ell,\sigma}\right]. \tag{A15}$$

Thus we obtain

$$Q_{4b} = Q'_{4b} + Q''_{4b} = -Q_{3a} + Q_2 + Q'_{\rm c}. \tag{A16}$$

Similarly Q_3 is written as

$$\begin{aligned} Q_3 &= Q_{3a} + \frac{B\hbar^2}{2m}\frac{1}{\beta}\sum_n \frac{1}{V}\sum_{\mathbf{k}q\sigma} k_z q |A_q|^2 [G_{\mathbf{k}-\frac{q}{2},n,\sigma} G_{\mathbf{k}-\frac{q}{2},n+\ell,\sigma} G_{\mathbf{k}+\frac{q}{2},n,-\sigma} + G_{\mathbf{k}-\frac{q}{2},n,\sigma} G_{\mathbf{k}-\frac{q}{2},n+\ell,\sigma} G_{\mathbf{k}+\frac{q}{2},n+\ell,-\sigma}] \\ &= Q_{3a} - 4Q_2 - 2Q_1 - Q'_{45}. \end{aligned} \tag{A17}$$

Adding the three equations (A9)(A16) and (A17), we finally obtain the result

$$Q_1 + Q_2 + Q_3 + Q_4 + Q_5 = Q_{\rm c} + Q'_{\rm c}. \tag{A18}$$

The term $Q'_{\rm c}$ is rewritten by use of partial integration over q as

$$\begin{aligned} Q'_{\rm c} &= \frac{B}{2}\frac{1}{\beta}\sum_n \frac{1}{V}\sum_{\mathbf{k}q\sigma} \sigma \Delta k_z |A_q|^2 \frac{1}{i\left(\omega_\ell + \Delta_{n\ell}\right)} \partial_q \left[G_{\mathbf{k}+\frac{q}{2},n,-\sigma} G_{\mathbf{k}-\frac{q}{2},n,\sigma} - G_{\mathbf{k}+\frac{q}{2},n+\ell,-\sigma} G_{\mathbf{k}-\frac{q}{2},n+\ell,\sigma}\right] \\ &= -\frac{B}{2}\frac{1}{\beta}\sum_n \frac{1}{V}\sum_{\mathbf{k}q\sigma} \sigma \Delta k_z (\partial_q |A_q|^2) \frac{1}{i\left(\omega_\ell + \Delta_{n\ell}\right)} \left[G_{\mathbf{k}+\frac{q}{2},n,-\sigma} G_{\mathbf{k}-\frac{q}{2},n,\sigma} - G_{\mathbf{k}+\frac{q}{2},n+\ell,-\sigma} G_{\mathbf{k}-\frac{q}{2},n+\ell,\sigma}\right]. \end{aligned} \tag{A19}$$

By use of (A3) and (A8) this becomes

$$Q'_{\rm c} = \frac{B}{2}\frac{1}{\beta}\sum_n \frac{1}{V}\sum_{\mathbf{k}q\sigma} (\partial_q |A_q|^2) \frac{\Delta\left(k_z + \frac{q}{2}\right)}{\Delta + \sigma\frac{(k_z + q/2)q}{m}} G_{\mathbf{k},n,\sigma} G_{\mathbf{k},n+\ell,\sigma}. \tag{A20}$$

APPENDIX B: CONDUCTIVITY CORRECTIONS $\delta\sigma$ AND σ'

First we calculated the conductivity correction due to the shift of the electron density. The correction to the electron density due to the interaction (8) is given by $\delta n \equiv \delta n_1 + \delta n_2$, where

$$\delta n_1 = \frac{\hbar^2}{4m}\frac{1}{\beta V}\sum_{\mathbf{k}qn\sigma} |A_q|^2 \frac{1}{2}(G_{\mathbf{k}n\sigma})^2, \tag{B1}$$

and

$$\delta n_2 = \frac{\hbar^2}{4m}\frac{1}{\beta V}\sum_{\mathbf{k}qn\sigma} |A_q|^2 \frac{\hbar^2 k_z^2}{m} (G_{\mathbf{k}-\frac{q}{2},n\sigma})^2 G_{\mathbf{k}+\frac{q}{2},n,-\sigma}. \tag{B2}$$

These contributions are shown diagramatically in Fig. 3. By use of (A8) the expression of δn_2 is simplified to be

$$\delta n_2 = -\frac{\hbar^2}{4m^2}\frac{1}{\beta V}\sum_{\mathbf{k}qn\sigma}|A_q|^2\frac{\left(k_z+\frac{q}{2}\right)^2}{2\sigma\Delta+\frac{(k_z+q/2)q}{m}}(G_{\mathbf{k},n\sigma})^2. \tag{B3}$$

The summation over ω_n is carried out as (see Appendix C)

$$\begin{aligned}\frac{1}{\beta}\sum_n (G_{\mathbf{k},n\sigma})^2 &= -\frac{1}{2\pi i}\int_{-\infty}^{\infty} dz f(z)\frac{i}{\tau}\frac{d}{dz}\frac{1}{(z-\epsilon_{\mathbf{k}\sigma})^2+\left(\frac{\hbar}{2\tau}\right)^2}\\ &= -\frac{1}{2\pi\tau}\frac{1}{\epsilon_{\mathbf{k}\sigma}^2+\left(\frac{\hbar}{2\tau}\right)^2}.\end{aligned} \tag{B4}$$

Thus we finally obtain

$$\delta n = -\frac{\hbar^3}{16\pi m\tau}\frac{1}{V}\sum_{\mathbf{k}q\sigma}\frac{|A_q|^2}{\epsilon_{\mathbf{k}\sigma}^2+\left(\frac{\hbar}{2\tau}\right)^2}\frac{\Delta-\sigma\frac{(k_z+q/2)k_z}{m}}{\Delta+\sigma\frac{(k_z+q/2)q}{2m}}. \tag{B5}$$

Thus the correction of the zeroth order conductivity, $\delta\sigma_{\rm c} = e^2\tau\delta n/m$ is obtained as

$$\delta\sigma_{\rm c} = -\frac{\hbar}{16\pi}\left(\frac{e\hbar}{m}\right)^2\frac{1}{V}\sum_{\mathbf{k}q\sigma}\frac{|A_q|^2}{\epsilon_{\mathbf{k}\sigma}^2+\left(\frac{\hbar}{2\tau}\right)^2}\frac{\Delta-\sigma\frac{(k_z+q/2)k_z}{m}}{\Delta+\sigma\frac{(k_z+q/2)q}{2m}}. \tag{B6}$$

The $\mathbf{k}$-summation is easily carried out by rewriting it by the energy integration to obtain

$$\delta\sigma_{\rm c} = -\frac{\hbar}{8}\left(\frac{e\hbar}{m}\right)^2\frac{1}{V}\sum_{q\sigma}N_\sigma\tau|A_q|^2\left\langle\frac{\Delta-\sigma\frac{(k_z+q/2)k_z}{m}}{\Delta+\sigma\frac{(k_z+q/2)q}{2m}}\right\rangle, \tag{B7}$$

where bracket denotes the angular average over $k_z \equiv k_{F\sigma}\cos\theta$.

Similarly the contribution $\sigma_{\rm c}'$, eq. (21), is calculated as

$$\sigma_{\rm c}' = \frac{\hbar}{8}\left(\frac{e\hbar}{m}\right)^2\frac{1}{V}\sum_{q\sigma}N_\sigma\tau|A_q|^2\left\langle\frac{\Delta\left(\Delta-\sigma\frac{(k_z+q/2)^2}{m}\right)}{\left[\Delta+\sigma\frac{(k_z+q/2)q}{2m}\right]^2}\right\rangle. \tag{B8}$$

From these expressions (B7) and (B8) it is seen that in the limit of $k_F\lambda \gg 1$ (i.e., $q \ll k_F$) and $\Delta \gg \hbar^2 k_F/m\lambda$, the sum of two terms vanishes; $\sigma_{\rm c}' + \delta\sigma_{\rm c} = 0$.

APPENDIX C: SUMMATION OVER ω_N IN EQ. (18)

The summation over Matsubara frequency, ω_n, in the expression of classical contribution to the conductivity, (18), can be carried out by use of contour integration as follows. The quantity we consider is

$$Q_{\rm c}(i\omega_\ell) = -B\frac{1}{V}\sum_{\mathbf{k}q\sigma}|A_q|^2 I_{\mathbf{k}q\sigma}(i\omega_\ell), \tag{C1}$$

where $B = ((e\hbar)^2/2m^2)$ and

$$I_{\mathbf{k}q\sigma}(i\omega_\ell) \equiv \frac{1}{\beta}\sum_n G_{\mathbf{k}-\frac{q}{2},n,\sigma}G_{\mathbf{k}-\frac{q}{2},n+\ell,\sigma}G_{\mathbf{k}+\frac{q}{2},n,-\sigma}G_{\mathbf{k}+\frac{q}{2},n+\ell,-\sigma}. \tag{C2}$$

This function is written by use of contour integration with respect to $z \equiv i\omega_n$ as

$$I_{\mathbf{k}q\sigma}(i\omega_\ell) = -\frac{1}{2\pi i}\oint_{C_0} dz f(z)G_{\mathbf{k}-\frac{q}{2},\sigma}(z)G_{\mathbf{k}-\frac{q}{2},\sigma}(z+i\omega_\ell)G_{\mathbf{k}+\frac{q}{2},-\sigma}(z)G_{\mathbf{k}+\frac{q}{2},-\sigma}(z+i\omega_\ell), \tag{C3}$$

where $f(z) \equiv 1/(1+e^{\beta z})$ and Green function $G_{\mathbf{k},\sigma,n}$ is here denoted by $G_{\mathbf{k},\sigma}(i\omega_n)$, and the contour C_0 goes around the imaginary axis in complex z-plane (Fig. 12). Noting that $G_{\mathbf{k},\sigma}(z) = [z + (1/2\tau)\mathrm{sgn}(\mathrm{Im}[z]) - \epsilon_{\mathbf{k},\sigma}]^{-1}$ has a cut

along $\mathrm{Im}[z]=0$, the contour can be changed to four paths C_1 parallel to the real axis, namely $z\equiv\pm(\omega'+i0)$ and $z\equiv-i\omega_\ell\pm(\omega'+i0)$, where ω' runs from $-\infty$ to ∞ (Fig. 12). We then obtain

$$\begin{aligned}I_{\mathbf{k}q\sigma}(i\omega_\ell)=-\frac{1}{\pi}\int_{-\infty}^{\infty}d\omega'\Bigg[&f(\omega')\frac{1}{(\omega'+i\omega_\ell+\frac{i\hbar}{2\tau}-\epsilon_{\mathbf{k}-\frac{q}{2},\sigma})}\frac{1}{(\omega'+i\omega_\ell+\frac{i\hbar}{2\tau}-\epsilon_{\mathbf{k}+\frac{q}{2},-\sigma})}\\&\times\mathrm{Im}\left(\frac{1}{(\omega'+\frac{i\hbar}{2\tau}-\epsilon_{\mathbf{k}-\frac{q}{2},\sigma})}\frac{1}{(\omega'+\frac{i\hbar}{2\tau}-\epsilon_{\mathbf{k}+\frac{q}{2},-\sigma})}\right)\\&+f(\omega'-i\omega_\ell)\frac{1}{(\omega'-i\omega_\ell-\frac{i\hbar}{2\tau}-\epsilon_{\mathbf{k}-\frac{q}{2},\sigma})}\frac{1}{(\omega'-i\omega_\ell-\frac{i\hbar}{2\tau}-\epsilon_{\mathbf{k}+\frac{q}{2},-\sigma})}\\&\times\mathrm{Im}\left(\frac{1}{(\omega'+\frac{i\hbar}{2\tau}-\epsilon_{\mathbf{k}-\frac{q}{2},\sigma})}\frac{1}{(\omega'+\frac{i\hbar}{2\tau}-\epsilon_{\mathbf{k}+\frac{q}{2},-\sigma})}\right)\Bigg].\end{aligned}\tag{C4}$$

The classical conductivity is expressed by taking the imaginary part of the correlation function analytically continued to $\omega+i0\equiv i\omega_\ell$ as

$$\sigma_{\mathrm{w}}=\lim_{\omega\to0}\mathrm{Im}\frac{Q_{\mathrm{w}}(\omega+i0)-Q_{\mathrm{w}}(i0)}{\omega}.\tag{C5}$$

The imaginary part of $I_{\mathbf{k}q\sigma}(i\omega_\ell=\omega+i0)$ is obtained from (C4) as

$$\begin{aligned}\mathrm{Im}I_{\mathbf{k}q\sigma}(\omega+i0)&=-\frac{1}{\pi}\int_{-\infty}^{\infty}d\omega'\mathrm{Im}\left(\frac{1}{(\omega'+\frac{i\hbar}{2\tau}-\epsilon_{\mathbf{k}-\frac{q}{2},\sigma})}\frac{1}{(\omega'+\frac{i\hbar}{2\tau}-\epsilon_{\mathbf{k}+\frac{q}{2},-\sigma})}\right)\\&\times\Bigg[f(\omega')\mathrm{Im}\left(\frac{1}{(\omega'+\omega+\frac{i\hbar}{2\tau}-\epsilon_{\mathbf{k}-\frac{q}{2},\sigma})}\frac{1}{(\omega'+\omega+\frac{i\hbar}{2\tau}-\epsilon_{\mathbf{k}+\frac{q}{2},-\sigma})}\right.\\&\left.-\ f(\omega'-\omega)\frac{1}{(\omega'-\omega+\frac{i\hbar}{2\tau}-\epsilon_{\mathbf{k}-\frac{q}{2},\sigma})}\frac{1}{(\omega'-\omega+\frac{i\hbar}{2\tau}-\epsilon_{\mathbf{k}+\frac{q}{2},-\sigma})}\right)\Bigg]\\&=-\frac{1}{\pi}\int_{-\infty}^{\infty}d\omega'\left[f(\omega')-f(\omega'+\omega)\right]\mathrm{Im}\left(\frac{1}{\omega'+\omega+\frac{i\hbar}{2\tau}-\epsilon_{\mathbf{k}-\frac{q}{2},\sigma}}\frac{1}{\omega'+\omega+\frac{i\hbar}{2\tau}-\epsilon_{\mathbf{k}+\frac{q}{2},-\sigma}}\right)\\&\times\mathrm{Im}\left(\frac{1}{\omega'+\frac{i\hbar}{2\tau}-\epsilon_{\mathbf{k}-\frac{q}{2},\sigma}}\frac{1}{\omega'+\frac{i\hbar}{2\tau}-\epsilon_{\mathbf{k}+\frac{q}{2},-\sigma}}\right).\end{aligned}\tag{C6}$$

By use of

$$f(\omega')-f(\omega'+\omega)=-\omega\frac{df(\omega')}{d\omega'}+O(\omega^2)\sim\omega\delta(\omega'),\tag{C7}$$

which holds at small ω and low temperature, we obtain

$$\mathrm{Im}I_{\mathbf{k}q\sigma}(\omega+i0)\sim-\frac{\omega}{\pi}\left[\mathrm{Im}\left(\frac{1}{\frac{i\hbar}{2\tau}-\epsilon_{\mathbf{k}-\frac{q}{2},\sigma}}\frac{1}{\frac{i\hbar}{2\tau}-\epsilon_{\mathbf{k}+\frac{q}{2},-\sigma}}\right)\right]^2.\tag{C8}$$

The classical contribution to the conductivity, (C5), is then obtained as

$$\sigma_{\mathrm{c}}=-\frac{\Delta^2\hbar^3}{8\pi\tau^2}\left(\frac{e\hbar}{m}\right)^2\frac{1}{V}\sum_{\mathbf{k}q\sigma}|A_q|^2\frac{(\epsilon_{\mathbf{k}-\frac{q}{2},\sigma}+\epsilon_{\mathbf{k}+\frac{q}{2},-\sigma})^2}{\left[(\epsilon_{\mathbf{k}-\frac{q}{2},\sigma})^2+\left(\frac{\hbar}{2\tau}\right)^2\right]^2\left[(\epsilon_{\mathbf{k}+\frac{q}{2},-\sigma})^2+\left(\frac{\hbar}{2\tau}\right)^2\right]^2}.\tag{C9}$$

APPENDIX D: DERIVATION OF EQ. (25) AND (29)

The $\mathbf{k}$-summation in (20) is carried out as follows. We neglect quantities of $O((q/k_F)^2)$ and approximate $\epsilon_{\mathbf{k}\pm q/2,\mp\sigma}\simeq\epsilon_{\mathbf{k}}\pm[(k_zq/2m)+\sigma\Delta]$. This is because the momentum transfer, q, is limited to a small value of $q\lesssim\lambda^{-1}$ due to the

form factor of the wall, $|A_q|^2 \propto [\cosh(\pi q\lambda/2)]^{-2}$, and we are considering the case of a thick wall, $k_F\lambda \gg 1$. Then $\sigma_{\rm w}$ is written as

$$\sigma_{\rm c} \simeq -\frac{\Delta^2\hbar^3}{8\pi\tau^2}\left(\frac{e\hbar}{m}\right)^2\frac{1}{V}\sum_q |A_q|^2 J_q, \tag{D1}$$

where

$$J_q \equiv \sum_{\mathbf{k}\sigma}\frac{4(\epsilon_{\mathbf{k}})^2}{\left[\left\{\epsilon_{\mathbf{k}}-\left(\frac{\hbar^2k_zq}{2m}+\sigma\Delta\right)\right\}^2+\left(\frac{\hbar}{2\tau}\right)^2\right]^2\left[\left\{\epsilon_{\mathbf{k}}+\left(\frac{\hbar^2k_zq}{2m}+\sigma\Delta\right)\right\}^2+\left(\frac{\hbar}{2\tau}\right)^2\right]^2}. \tag{D2}$$

This function is written as

$$\begin{aligned} J_q &\equiv 2\int_{-1}^{1}\frac{d\cos\theta}{2}\int_{-\epsilon_F}^{\infty}d\epsilon N(\epsilon)\frac{4\epsilon^2}{\left[\left\{\epsilon-\left(\frac{\hbar^2kq\cos\theta}{2m}+\Delta\right)\right\}^2+\left(\frac{\hbar}{2\tau}\right)^2\right]^2\left[\left\{\epsilon+\left(\frac{\hbar^2kq\cos\theta}{2m}+\Delta\right)\right\}^2+\left(\frac{\hbar}{2\tau}\right)^2\right]^2} \\ &\equiv \int_{-1}^{1}d\cos\theta\int_{-\epsilon_F}^{\infty}d\epsilon N(\epsilon)F_\theta(\epsilon), \end{aligned} \tag{D3}$$

where $N(\epsilon) \equiv (Vm^{3/2}/\pi^2\sqrt{2}\hbar^3)\sqrt{\epsilon+\epsilon_F}$ is the density of states, and $k \equiv \sqrt{2m(\epsilon+\epsilon_F)}/\hbar$, θ being the angle between $\mathbf{k}$ and the z-axis, and $F_\theta(\epsilon)$ is defined by the last line. In the first line we have included the factor of two due to the summation over the spin. The integration over ϵ can be carried out by use of contour integration. In doing this we need to be a little bit careful since the density of states in three-dimensions $N(\epsilon) \propto \sqrt{\epsilon+\epsilon_F}$ has a cut on the real axis running from $\epsilon = -\epsilon_F$ to $\epsilon = \infty$. Choosing a closed path C_2 in the ϵ-plane as in Fig. 13, the ϵ-integral in (D3) is written as

$$\int_{-\epsilon_F}^{\infty}d\epsilon N(\epsilon)F_\theta(\epsilon) = \frac{1}{2}\oint_{C_2}d\epsilon N(\epsilon)F_\theta(\epsilon). \tag{D4}$$

The contour C_2 contains four poles at $\epsilon = \epsilon^*_{\sigma,\pm} \equiv \sigma\left(\Delta+\frac{\hbar^2k(\epsilon^*_\sigma)q}{2m}\cos\theta\right) \pm i\frac{\hbar}{2\tau}$. In ferromagnets with strong polarization we are interested in, $\Delta \sim O(\epsilon_F)$, and then neglecting $O(q/k_F)$ contributions we may approximate $\epsilon^*_{\sigma,\pm} \sim \sigma\left(\Delta+\frac{\hbar^2k_{F\sigma}q}{2m}\cos\theta\right) \pm i\frac{\hbar}{2\tau}$, where $\hbar k_{F\sigma} \equiv \sqrt{2m(\epsilon_F+\sigma\Delta)}$ is the Fermi momentum of the polarised electron. The density of states estimated at the pole in the lower half plane, $\epsilon^*_{\sigma,-}$, has a opposite sign as the upper half plane, i.e., $N(\epsilon^*_{\sigma,\pm}) \sim \pm N(\sigma\Delta) \equiv \pm N_\sigma$. We therefore obtain

$$\int_{-\epsilon_F}^{\infty}d\epsilon N(\epsilon)F_\theta(\epsilon) \simeq 2\pi\left(\frac{\tau}{\hbar}\right)^3\sum_\sigma N_\sigma\frac{1}{\left(\frac{\hbar^2k_{F\sigma}q}{2m}\cos\theta+\sigma\Delta\right)^2+\left(\frac{\hbar}{2\tau}\right)^2}, \tag{D5}$$

where $N_\sigma \equiv (Vmk_{F\sigma}/2\pi^2\hbar^2)$. The integration over $\cos\theta$ in eq. (D3) is then easily carried out to obtain

$$J_q = \frac{2m^2V\tau^4}{\pi\hbar^8}\sum_\sigma\frac{1}{q}\left[\tan^{-1}\frac{2\tau}{\hbar}\left(\frac{\hbar^2k_{F\sigma}q}{2m}+\Delta\right)+\tan^{-1}\frac{2\tau}{\hbar}\left(\frac{\hbar^2k_{F\sigma}q}{2m}-\Delta\right)\right]. \tag{D6}$$

The conductivity (D1) is then obtained by use of the expression of A_q, eq. (9), ($\sum_q |A_q|^2\cdots = (\pi/L)\int dq[\cosh^2(\pi q\lambda/2)]^{-1}\cdots$) as

$$\sigma_{\rm c} = -\frac{e^2\Delta^2\tau^2}{8\pi\hbar^3L}\sum_\sigma\int_{-\infty}^{\infty}\frac{dq}{q}\frac{1}{\cosh^2\frac{\pi}{2}q\lambda}\left[\tan^{-1}\frac{2\tau}{\hbar}\left(\frac{\hbar^2k_{F\sigma}q}{2m}+\Delta\right)+\tan^{-1}\frac{2\tau}{\hbar}\left(\frac{\hbar^2k_{F\sigma}q}{2m}-\Delta\right)\right]. \tag{D7}$$

Changing the variable $x \equiv \pi\lambda q/2$ we obtain (25).

To look into the asymptotic behaviors at large Δ it is useful to rewrite the result by use of $\tan^{-1}x = \pm\pi/2 - \tan^{-1}(1/x)$ for $x > (<)0$ as

$$\sigma_{\rm c} = -\frac{e^2}{4\pi\hbar}\tilde{\Delta}^2n_{\rm w}\sum_\sigma\left[\pi\int_{\Lambda_\sigma}^{\infty}\frac{dx}{x}\frac{1}{\cosh^2x}+\int_0^{\infty}\frac{dx}{x}\frac{1}{\cosh^2x}\tan^{-1}\frac{2\tilde{l_\sigma}x}{(2\tilde{\Delta})^2-(\tilde{l_\sigma}x)^2+1}\right], \tag{D8}$$

where $\tilde{\Delta} \equiv \Delta\tau/\hbar$, $\tilde{l_\sigma} \equiv (2l_\sigma/\pi\lambda)$, and $\Lambda_\sigma \equiv 2\tilde{\Delta}/\tilde{l_\sigma} = (\pi m\Delta\lambda/k_{F\sigma}\hbar^2)$. We consider the case $\tilde{\Delta} \gg 1$ and $\Lambda_\sigma \gg 1$, which would be satisfied for d electrons in $3d$ transition metals. In this case the inequality $(\tilde{\Delta})^2 \gg (\tilde{l_\sigma})^2, \tilde{l_\sigma}$ is satisfied if Δ/ϵ_F is not too small. Then the conductivity correction is approximated as

$$\begin{aligned}\sigma_{\rm c} &= -\frac{e^2}{4\pi\hbar}\tilde{\Delta}^2 n_{\rm w}\sum_\sigma\left[4\pi\int_{\Lambda_\sigma}^\infty\frac{dx}{x}e^{-2x}+\frac{\tilde{l_\sigma}}{2\tilde{\Delta}^2}\right]\int_0^\infty\frac{dx}{\cosh^2 x}\\ &= -\frac{e^2}{4\pi^2\hbar}\frac{\Delta\tau^2}{m\lambda}n_{\rm w}\sum_\sigma k_{F\sigma}\left[2\pi e^{-2\Lambda_\sigma}+\frac{\hbar}{\Delta\tau}\right].\end{aligned} \tag{D9}$$

In the case of a thick wall ($\lambda \gg k_F^{-1}$) with a finite τ, the first term in (D9) is exponentially small and thus neglected. The conductivity in this case is

$$\sigma_{\rm c} \simeq -\frac{e^2}{8\pi\hbar}n_{\rm w}\sum_\sigma\tilde{l_\sigma}\int_0^\infty\frac{dx}{\cosh^2 x} = -\frac{e^2}{8\pi\hbar}n_{\rm w}\sum_\sigma\tilde{l_\sigma}\quad(\Delta\tau/\hbar, m\Delta\lambda/k_{F\sigma}\hbar^2 \gg 1). \tag{D10}$$

On the other hand if we take the limit of $\tau\to\infty$ first, the first term in (D9) becomes dominant and the result of Mori formula (eq. (35)) is obtained. The result of Cabrera and Falicov [19], obtained by calculating the reflection coefficient in the absence of impurities, corresponds to this limit.

APPENDIX E: COOPERONS IN FERROMAGNETS

In this section we calculate the quantum correction to the conductivity in terms of the particle-particle ladder amplitude (Cooperon). In this section we discuss the Cooperon in ferromagnets with $\Delta\tau/\hbar \gg 1$, taking into account the impurity scattering (eq. (2)) but in the absence of domain wall. Let us consider a correlation function

$$\begin{aligned}&<< c^\dagger_{\mathbf{k},n,\sigma}c_{-\mathbf{k}'+\mathbf{q},n',\sigma'}c^\dagger_{-\mathbf{k}+\mathbf{q},n',\sigma'}c_{\mathbf{k}',n,\sigma} >>=< c^\dagger_{\mathbf{k},n,\sigma}c_{-\mathbf{k}'+\mathbf{q},n',\sigma'}c^\dagger_{-\mathbf{k}+\mathbf{q},n',\sigma'}c_{\mathbf{k}',n,\sigma} >\\ &\quad+\frac{1}{2}\sum_{\mathbf{k}_1,\mathbf{k}_2,\mathbf{q}'}v^2 < \sum_{i,j}e^{i\mathbf{q}'(\mathbf{X}_i-\mathbf{X}_j)} >_{\rm imp}\\ &\quad\times < c^\dagger_{\mathbf{k},n,\sigma}c_{-\mathbf{k}'+\mathbf{q},n',\sigma'}c^\dagger_{-\mathbf{k}+\mathbf{q},n',\sigma'}c_{\mathbf{k}',n,\sigma}c^\dagger_{\mathbf{k}_1,n,\sigma}c_{\mathbf{k}_2,n,\sigma}c^\dagger_{-\mathbf{k}_1+\mathbf{q}',n',\sigma'}c_{-\mathbf{k}_2+\mathbf{q}',n',\sigma'} > +\cdots\\ &\equiv -(G_{\mathbf{k},n,\sigma}G_{-\mathbf{k}+\mathbf{q},n',\sigma'}\delta_{\mathbf{k},\mathbf{k}'}+\Gamma^{\sigma\sigma'}_{nn'}(\mathbf{k},\mathbf{k}',\mathbf{q})G_{\mathbf{k},n,\sigma}G_{\mathbf{k}',n,\sigma}G_{-\mathbf{k}'+\mathbf{q},n',\sigma'}G_{-\mathbf{k}+\mathbf{q},n',\sigma'}),\end{aligned} \tag{E1}$$

where we have treated the impurity perturbatively and double bracket denotes averaging over the electron states and impurities, $<>_{\rm imp}$ being the average over impurity. (In taking the impurity average, the self-energy processes are not included since they are already taken into account as a lifetime τ of the Green function.) The function $\Gamma^{\sigma\sigma'}_{nn'}$ is defined by the last line and Cooperon denotes the singular part of $\Gamma^{\sigma\sigma'}_{nn'}$ for $q\sim 0$, which is calcualted below. By use of eq. (E1) the current correlation function, eq. (13), which is related to the conductivity, is expressed as

$$\begin{aligned}Q(i\omega_\ell) &= -\left(\frac{e\hbar}{m}\right)^2\frac{\hbar}{V\beta}\sum_{n\mathbf{k}\sigma}\Big[k_z^2 G_{\mathbf{k}n\sigma}G_{\mathbf{k},n+\ell,\sigma}\\ &\qquad+\sum_{\mathbf{q}}k_z(-k+q)_z G_{\mathbf{k},n,\sigma}G_{\mathbf{k},n+\ell,\sigma}G_{-\mathbf{k}+\mathbf{q},n,\sigma}G_{-\mathbf{k}+\mathbf{q},n+\ell,\sigma}\Gamma^{\sigma\sigma}_{n,n+\ell}(\mathbf{k}'=-\mathbf{k}+\mathbf{q},\mathbf{q})\Big]\\ &\equiv Q_0+Q_{0\rm q}.\end{aligned} \tag{E2}$$

The first term, Q_0 corresponds to the Boltzmann conductivity and the second term $Q_{0\rm q}$ (described in Fig. 5) turns out to describe the quantum effect. If the electron elastic mean free path is long (i.e., low impurity density) the second contribution $Q_{0\rm q}$ is small but as $k_F l$ becomes smaller the this term becomes important (see in eq. (E10)).

We now show that $\Gamma^{\sigma\sigma}_{n,n+\ell}(\mathbf{k}'=-\mathbf{k}+\mathbf{q},\mathbf{q})$ contains a singular contribution at small $\mathbf{q}$, which indicates the enhancement of the backward scattering due to the coherence, namely the weak localization of electron. Cooperon denotes this singular contribution and is calcualted by summing over the ladder contribution shown in Fig. 4(a). (There is another contribution to Γ which is singular for $\mathbf{q}\sim\mathbf{k}+\mathbf{k}'$, called a diffuson, represented by the diagram in Fig. 4(b), but we do not consider this process since it does not contribute to the conductivity because of the current vertex.) The result of Cooperon is (we write $\Gamma^{\sigma\sigma}_{n,n+\ell}(\mathbf{k}'=-\mathbf{k}+\mathbf{q},\mathbf{q})$ simply as $\Gamma^{\sigma\sigma}_{n,n+\ell}(\mathbf{q})$ below)

$$\Gamma^{\sigma\sigma'}_{nn'}(\mathbf{q}) = n_{\rm i}v^2\left[1 + n_{\rm i}v^2 I^{\sigma\sigma'}_{nn'}(\mathbf{q}) + (n_{\rm i}v^2 I^{\sigma\sigma'}_{nn'}(\mathbf{q}))^2 + \cdots\right] \simeq \frac{n_{\rm i}v^2}{1 - n_{\rm i}v^2 I^{\sigma\sigma'}_{nn'}(\mathbf{q})}, \tag{E3}$$

where

$$I^{\sigma\sigma'}_{nn'}(\mathbf{q}) \equiv \sum_{\mathbf{k}} G_{\mathbf{k},n,\sigma} G_{-\mathbf{k}+\mathbf{q},n',\sigma'}. \tag{E4}$$

We consider the important case of small q ($q \lesssim l^{-1}$) , and then this function can be expanded with respect to q as

$$I^{\sigma\sigma'}_{nn'}(\mathbf{q}) \simeq \sum_{\mathbf{k}} \left[G_{\mathbf{k},n,\sigma} G_{\mathbf{k},n',\sigma'} - \left(\frac{\hbar^2 k_z q}{2m}\right)^2 \left\{ (G_{\mathbf{k},n,\sigma} G_{\mathbf{k},n',\sigma'})^2 - G_{\mathbf{k},n,\sigma}(G_{\mathbf{k},n',\sigma'})^3 - (G_{\mathbf{k},n,\sigma})^3 G_{\mathbf{k},n',\sigma'} \right\} \right]. \tag{E5}$$

The summation over $\mathbf{k}$ can be written in terms of the integration over the energy, ϵ, from $-\epsilon_F$ to the infinity, and this integral is carried out in the same way as in eq. (D3). The first term of (E5)is calculated as

$$\begin{aligned} I^{(1)\sigma\sigma'}_{+-} &\equiv \sum_{\mathbf{k}} G_{\mathbf{k},n>0,\sigma} G_{\mathbf{k},n<0,\sigma'} \\ &= \int_{-\epsilon_F}^{\infty} d\epsilon N(\epsilon) \frac{1}{\left[i\hbar\left(\frac{1}{2\tau} + \omega_n\right) - \epsilon + \sigma\Delta\right]} \frac{1}{\left[-i\hbar\left(\frac{1}{2\tau} - \omega_{n'}\right) - \epsilon + \sigma'\Delta\right]} \\ &\simeq \frac{2\pi i}{(\sigma - \sigma')\Delta + i\hbar\left(\frac{1}{\tau} + \omega_n - \omega_{n'}\right)} N(0), \end{aligned} \tag{E6}$$

where we have neglected higher order of $O(\epsilon_F\tau/\hbar)^{-1}$ and $O(\Delta/\epsilon_F)$. It is seen from this result that for the electrons with the same spin ($\sigma = \sigma'$), $I^{(1)\sigma\sigma}_{+-} \simeq 2\pi N\tau/\hbar[1 - (\omega_n - \omega_{n'})\tau] + O((\omega_n - \omega_{n'})\tau)^2$ is large but for $\sigma = -\sigma'$, $I^{(1)\sigma,-\sigma}_{+-}$ is smaller by a factor of $(\Delta\tau/\hbar)^{-1}$. In the case of $\sigma = \sigma'$ other terms in eq. (E5) are calculated to obtain

$$I^{\sigma\sigma}_{+-}(\mathbf{q}) \simeq 2\pi N \frac{\tau}{\hbar}[1 - (Dq^2 + \omega_n - \omega_{n'})\tau], \tag{E7}$$

where $D \equiv [(\hbar k_F)^2\tau/3m^2]$. In this case the sum of the ladder (E3) turns out to be singular at low energy (by use of $2\pi n_{\rm i}v^2 N(0)\tau/\hbar = 1$);

$$\Gamma^{\sigma\sigma}_{+-} \simeq \frac{n_{\rm i}v^2}{[Dq^2 + \omega_n - \omega_{n'}]\tau}. \tag{E8}$$

This singular behavior indicates the enhancement of the backward scattering amplitude due to the quantum interference [32,33]. On the other hand if $\sigma = -\sigma'$, $I^{\sigma,-\sigma}$ is small and thus $\Gamma^{\sigma,-\sigma}_{+-}$ is not important. For the case of both n and n' are positive or negative, it is easy to sea that the ϵ-integral that corresponds to eq. (E6) vanishes. Therefore $\Gamma^{\sigma\sigma'}_{nn'}$ is important only if $nn' < 0$ and $\sigma = \sigma'$. Other contributions are neglected below.

By use of (E2) and (E8), we obtain the quantum correction to the conductivity as

$$\begin{aligned} \sigma_{0\rm q} &= -\frac{1}{2\pi}\left(\frac{e\hbar}{m}\right)\frac{1}{V}\frac{4\pi\hbar k_F^2}{3}N(0)\left(\frac{\tau}{\hbar}\right)^3 \sum_{\mathbf{q},\sigma}\Gamma^{\sigma\sigma}_{+-} \\ &= -\frac{2}{3\pi}\frac{e^2}{\hbar}\ell^2\frac{1}{V}\sum_{\mathbf{q}}\frac{1}{Dq^2\tau}. \end{aligned} \tag{E9}$$

In three-dimensions, $\frac{1}{V}\sum_{\mathbf{q}}\frac{1}{Dq^2\tau} \simeq \frac{3}{2\pi^2}\int_{L^{-1}}^{\ell^{-1}}\frac{dq}{\ell^2} = \frac{3}{2\pi^2\ell^3}$ and thus the ratio to the classical conductivity is obtained as

$$\frac{\sigma_{0\rm q}}{\sigma_0} = -\frac{3}{\pi}\frac{1}{(k_F\ell)^2} = -\frac{3}{4\pi}\left(\frac{\hbar}{\epsilon_F\tau}\right)^2. \tag{E10}$$

One can see that $\sigma_{0\rm q}$ is a "quantum" correction, which vanishes in the limit of $\hbar \to 0$.

APPENDIX F: SUMMATION OVER MATSUBARA FREQUENCY IN EQ. (68)

Here we will carry out the summation over Matsubara frequencies in eq. (68),

$$J \equiv \frac{1}{\beta^2}{\sum_{n,n'}}'(\tilde{\Gamma}_0(q,|n+l-n'|))^2(\tilde{\Gamma}_0(q,|n-(n'+\ell')|))^2$$
$$= \frac{1}{\beta^2}\sum_{n,n'}\frac{1}{(Dq^2+|\omega_{n+\ell}-\omega_{n'}|)^2(Dq^2+|\omega_n-\omega_{n'+\ell'}|)^2}. \tag{F1}$$

The summation here $\sum'_{n,n'}$ is restricted to the following three cases, where the Cooperons becomes important at small q;

$$\begin{array}{ll} \text{I}: & n+\ell, n>0, \quad n'+\ell', n'<0 \\ \text{II}: & n+\ell, n<0, \quad n'+\ell', n'>0 \\ \text{III}: & n+\ell, n'+\ell'>0, \quad n, n'<0. \end{array} \tag{F2}$$

Firstly the contribution from the case I is written as

$$J_{\rm I} = \frac{1}{\beta^2}\sum_{n=0}^{\infty}\sum_{n'=-\infty}^{-\ell'}\frac{1}{(Dq^2+\omega_{n+\ell}-\omega_{n'})^2(Dq^2+\omega_n-\omega_{n'+\ell'})^2}$$
$$= \frac{1}{\beta^2}\sum_{n=0}^{\infty}\sum_{n''\equiv-(n'+\ell')=0}^{\infty}\frac{1}{(Dq^2+\omega_{n+\ell}+\omega_{n''+\ell'})^2(Dq^2+\omega_n+\omega_{n''})^2}. \tag{F3}$$

We are interested in only the term proportional to $\omega_\ell\omega_{\ell'}$. Expanding $1/(Dq^2+\omega_{n+\ell}+\omega_{n''+\ell'})^2$ with respect to ω_ℓ and $\omega_{\ell'}$ we obtain this term as

$$J_{\rm I} \simeq \omega_\ell\omega_{\ell'}\frac{1}{\beta^2}\sum_{n=0}^{\infty}\sum_{n''=0}^{\infty}\frac{1}{(Dq^2+\omega_n+\omega_{n''})^6}. \tag{F4}$$

The contribution from case II turns out to be the same; $J_{\rm II} = J_{\rm I}$. Case III is treated as follows.

$$J_{\rm III} = \frac{1}{\beta^2}\sum_{n=-\ell}^{0}\sum_{n'=-\ell'}^{0}\frac{1}{(Dq^2+\omega_{n+\ell}-\omega_{n'})^2(Dq^2+\omega_{n'+\ell'}-\omega_n)^2}$$
$$= \frac{1}{\beta^2}\sum_{n''\equiv-n=0}^{\ell}\sum_{n'''\equiv n'+\ell'=0}^{\ell'}\frac{1}{(Dq^2-\omega_{n''-\ell}-\omega_{n'''-\ell'})^2(Dq^2+\omega_{n''}+\omega_{n'''})^2}. \tag{F5}$$

By use of $\sum_{n=0}^{\ell}F(n) = \sum_{n=0}^{\infty}(F(n)-F(n+\ell))$ ($F(n)$ being any function) we obtain

$$J_{\rm III} = \frac{1}{\beta^2}\sum_{n\equiv=0}^{\infty}\sum_{n'=0}^{\infty}\Bigg[\frac{1}{(Dq^2-(\omega_n+\omega_{n'})+\omega_{\ell+\ell'})^2(Dq^2+\omega_n+\omega_{n'})^2}$$
$$-\frac{1}{(Dq^2-(\omega_n+\omega_{n'})+\omega_{\ell'})^2(Dq^2+\omega_n+\omega_{n'}+\omega_\ell)^2}$$
$$-\frac{1}{(Dq^2-(\omega_n+\omega_{n'})+\omega_\ell)^2(Dq^2+\omega_n+\omega_{n'}+\omega_{\ell'})^2}$$
$$+\frac{1}{(Dq^2-(\omega_n+\omega_{n'}))^2(Dq^2+\omega_n+\omega_{n'}+\omega_{\ell+\ell'})^2}\Bigg]. \tag{F6}$$

Taking the term proportional to $\omega_\ell\omega_{\ell'}$ we obtain $J_{\rm III} \simeq \omega_\ell\omega_{\ell'}J'_6$ where J'_6 is defined in eq. (73). Adding these results we obtain eq. (71).

APPENDIX G: CALCULATION OF DIAGRAMS WITH FIVE AND SIX COOPERONS

Here the processes containing five and six Cooperons (eqs. (76)(77)) are calculated. Firstly let us evaluated the diagram Fig. 10(a). There are three different contributions shown in Fig. 10(a-(i-iii)) with different configuration of $\delta\Gamma_{\rm w}$ and Γ. The diagram Fig. 10(a-i) is calculated as

$$\begin{aligned}F_{\rm 5a(i)} = \left(\frac{e\hbar}{m}\right)^4 \frac{1}{V^2}\sum_{\mathbf{k},\mathbf{k}',\mathbf{k}'',\mathbf{q},\sigma}\frac{1}{\beta^2}\sum_{n,n'}{}' k_z(-k+q)_z k'_z(-k''+q)_z G_{\mathbf{k},n+\ell,\sigma}G_{\mathbf{k},n,\sigma}G_{-\mathbf{k}+\mathbf{q},n'+\ell',\sigma}G_{-\mathbf{k}+\mathbf{q},n',\sigma}\\ \times G_{\mathbf{k}',n+\ell,-\sigma}G_{\mathbf{k}',n,-\sigma}G_{-\mathbf{k}'+\mathbf{q},n',-\sigma}G_{\mathbf{k}'',n,-\sigma}G_{-\mathbf{k}''+\mathbf{q},n',-\sigma}G_{-\mathbf{k}''+\mathbf{q},n'+\ell',-\sigma}\\ \times\delta\Gamma_{\rm w}(q,|n+\ell-n'|)\delta\Gamma_{\rm w}(q,|n-(n'+\ell')|)\Gamma(q,|n-n'|).\end{aligned} \tag{G1}$$

Here the summation $\sum'_{n,n'}$ is carried out in the two cases,

$$\begin{aligned}&{\rm I}: \ \ n+\ell, n>0, \ \ n'+\ell', n'<0\\ &{\rm II}: \ \ n+\ell, n<0, \ \ n'+\ell', n'>0.\end{aligned} \tag{G2}$$

Summation over $\mathbf{k}'$ and $\mathbf{k}''$ gives rise to a contribution small at $q\to 0$;

$$\begin{aligned}\sum_{\mathbf{k}'} k'_z G_{\mathbf{k}',n+\ell,-\sigma}G_{\mathbf{k}',n,-\sigma}G_{-\mathbf{k}'+\mathbf{q},n',-\sigma} &\simeq \sum_{\mathbf{k}'} k'_z G_{\mathbf{k}',n+\ell,-\sigma}G_{\mathbf{k}',n,-\sigma}G_{\mathbf{k}',n',-\sigma}\left[1-\frac{\hbar^2(\mathbf{k}'\cdot\mathbf{q})}{m}G_{\mathbf{k}',n',-\sigma}\right]\\ &= -\frac{\hbar^2}{m}q_z\sum_{\mathbf{k}'}k'_z G_{\mathbf{k}',n+\ell,-\sigma}G_{\mathbf{k}',n,-\sigma}(G_{\mathbf{k}',n',-\sigma})^2,\\ &\simeq -\frac{q_z}{m\hbar}\frac{4\pi}{3}k_F^2 N(0)\tau^3,\end{aligned} \tag{G3}$$

for both cases I and II (in the last line we have neglected quantities of $O(\Delta/\epsilon_F)^2$). We thus obtain for case I

$$\begin{aligned}F_{\rm 5a(i)I} \simeq -F_0\frac{2k_F^2q_z^2}{3m^2\tau^3}w\left(\frac{r}{\lambda}\right)^2\\ \times\sum_{n=0}^{\infty}\sum_{n'=-\infty}^{-\ell'}\frac{1}{(Dq^2+\omega_{n+\ell}-\omega_{n'})^2}\frac{1}{(Dq^2+\omega_n-\omega_{n'+\ell'})^2}\frac{1}{(Dq^2+\omega_n-\omega_{n'})}.\end{aligned} \tag{G4}$$

By similar calculation as in Appendix F and by use of $D\equiv\hbar^{2k_F^2}\tau/(3m^2)$, the term linear in both ω_ℓ and $\omega_{\ell'}$ of $F_{\rm 5a(i)I}$ results in

$$\frac{F_{\rm 5a(i)I}}{\omega_\ell\omega_{\ell'}} \simeq -F_0[W\,(r/\lambda)]^2\frac{2Dq_z^2}{\tau^4}8J_7. \tag{G5}$$

Similarly, other contributions are calculated and the result of $F_{\rm 5a}\equiv\sum_{\alpha={\rm I,II}}F_{\rm 5a(i)\alpha}+\sum_{\alpha={\rm I,II}}F_{\rm 5a(ii)\alpha}+\sum_{\alpha={\rm I,II}}F_{\rm 5a(iii)\alpha}$ is obtained as

$$\begin{aligned}\frac{F_{\rm 5a}}{\omega_\ell\omega_{\ell'}} &\simeq -F_0[W\,(r/\lambda)]^2\frac{2Dq_z^2}{\tau^4}J_7\left[(8+8)+(4+10)+(10+4)\right]\\ &= -F_0[W\,(r/\lambda)]^2\frac{2Dq_z^2}{\tau^4}44J_7.\end{aligned} \tag{G6}$$

Diagram (a') is calculated as

$$\begin{aligned}\frac{F_{\rm 5a'}}{\omega_\ell\omega_{\ell'}} &\simeq -F_0[W\,(r/\lambda)]^2\frac{2Dq_z^2}{\tau^4}J_7\left[4+10+2+2+14+14\right]\\ &= -F_0[W\,(r/\lambda)]^2\frac{2Dq_z^2}{\tau^4}46J_7.\end{aligned} \tag{G7}$$

Other diagrams (b)(c)(d) give rise to the same contributions as (a)+(a') and so the result of five Cooperons processes are obtained as

$$\frac{F_5}{\omega_\ell\omega_{\ell'}} \simeq -F_0[W(r/\lambda)]^2\frac{2Dq_z^2}{\tau^4}J_7(44+46)\times 4$$
$$= -F_0[W(r/\lambda)]^2 720\frac{Dq_z^2}{\tau^4}J_7. \tag{G8}$$

Diagrams of six Cooperons in Fig. 11 are calculated in the same way. For example, diagram (a) leads to

$$\frac{F_{6a}}{\omega_\ell\omega_{\ell'}} \simeq -F_0[W(r/\lambda)]^2\frac{(2Dq_z^2)^2}{\tau^4}J_8(14+7+10+11+14+7)\times 2$$
$$= -F_0[W(r/\lambda)]^2\frac{(2Dq_z^2)^2}{\tau^4}126J_8. \tag{G9}$$

Here bracket denotes the summation over six different ways of putting two $\delta\Gamma$'s and two Γ's. Two factors of 2 in the first line are due to the two cases I and II. There are other processes with different arrangement of n' and $n'+\ell'$, corresponding to (a') in Fig. 8, which give the equal contribution.Thus

$$\frac{F_{6aa'}}{\omega_\ell\omega_{\ell'}} = -F_0[W(r/\lambda)]^2\frac{(2Dq_z^2)^2}{\tau^4}252J_8. \tag{G10}$$

It turns out that (b),(c) leads to the same contribution and thus we obtain

$$\frac{F_6}{\omega_\ell\omega_{\ell'}} \simeq -F_0[W(r/\lambda)]^2\frac{(Dq_z^2)^2}{\tau^4}3024J_8. \tag{G11}$$

APPENDIX H: CALCULATION OF J_M AND J_6'

The summation over the Matsubara frequency in the expression of J_m and J_6', eqs. (72) and (73) is carried out here. J_m can be written by use of contour integration as

$$J_m = \frac{1}{\beta^2}\sum_{n,n'=0}^{\infty}\frac{1}{(D\mathbf{q}^2+\omega_n+\omega_{n'})^m}$$
$$= \left(\frac{-1}{2\pi i}\right)^2\int_{C_+}dz\int_{C_+}dz' f(z)f(z')\frac{1}{[Dq^2-i(z+z')]^m}$$
$$= -\left(\frac{1}{2\pi}\right)^2\int_{-\infty}^{\infty}dz\int_{-\infty}^{\infty}dz' f(z)f(z')\frac{1}{[Dq^2-i(z+z'+i0)]^m}, \tag{H1}$$

where C_+ denotes the contour which surrounds the imaginary axis in the upper-half z-plane, and we have deformed the path to the path just above the real axis. By use of partial integration we obtain

$$J_m = \left(\frac{1}{2\pi}\right)^2\frac{1}{(m-1)(m-2)}\int_{-\infty}^{\infty}dz\int_{-\infty}^{\infty}dz'\frac{df(z)}{dz}\frac{df(z')}{dz'}\frac{1}{[Dq^2-i(z+z'+i0)]^{m-2}}$$
$$= \left(\frac{1}{2\pi}\right)^2\frac{1}{(m-1)(m-2)}\frac{1}{(Dq^2)^{m-2}}. \tag{H2}$$

Similarly J_6' is written as

$$J_6' = \left(\frac{1}{2\pi}\right)^2\int_{-\infty}^{\infty}dz\int_{-\infty}^{\infty}dz' f(z)f(z')\frac{d^2}{dzdz'}\left[\frac{1}{[Dq^2-i(z+z')]^2[Dq^2+i(z+z')]^2}\right]$$
$$= \left(\frac{1}{2\pi}\right)^2\frac{1}{(Dq^2)^4}. \tag{H3}$$

[1] W. Thomson: Proc. Royal Soc. London **8** (1857) 546.
[2] J. Smit: Physica **XVI** (1951) 612.
[3] T. R. McGuire and R. I. Potter: IEEE Trans. Magn. **MAG-11** (1975) 1018.
[4] There has been, however, some exceptions; e.g., negative $\Delta\rho_{\rm ani}$ has recently been observed in Fe wire [5].
[5] A. D. Kent, U. Ruediger, J. Y. S. Zhang, P. M. Levy and S. S. P. Parkin: IEEE Transactions on Magnetics (Fall 1998).
[6] S. Y. Hsu, A. Barthèlèmy, P. Holody, R. Loloee, P. A. Schoeder and A. Fert: Phys. Rev. Lett. **78** (1997) 2652.
[7] T. Ono, H. Miyajima, K. Shigeto, K. Mibu, N. Hosoito and T. Shinjo, to appear in Science (1999).
[8] H. Barkhausen: Phys. Z. **20** (1919) 401.
[9] N. Giordano and J. D. Monnier, Physica **B194-196** (1994) 1009.
[10] K. Hong and N. Giordano: Phys. Rev. **B51**(1995) 9855; J. Phys. CM**8** (1996) 301.
[11] K. Hong and N. Giordano: Euro. Phys. Lett. **36** (1996) 147.
[12] K. Hong and N. Giordano: J. Phys. CM**10** (1998) L401.
[13] Y. Otani, K. Fukamichi, O. Kitakami, Y. Shimada, B. Pannetier, J. P. Nozieres, T. Matsuda and A. Tonomura: Proc. MRS Spring Meeting, San Francisco, 1997.
[14] U. Ruediger, J. Y. S. Zhang, A. D. Kent and S. S. P. Parkin: Phys. Rev. Lett. **80** (1998) 5639.
[15] U. Ruediger, J. Yu, S. S. P. Parkin, A. D. Kent: to appear in Journal of Magnetism and Magnetic Materials.
[16] U. Ruediger, J. Yu, L. Thomas, S. S. P. Parkin, A. D. Kent: preprint cond-mat 9901245.
[17] Y. Otani, private communication.
[18] J. F. Gregg et al.: Phys. Rev. Lett. **77**(1996) 1580.
[19] G. G. Cabrera and L. M. Falicov: Phys. Stat. Sol. (b)**61** (1974) 539.
[20] P. Schiffer, A. P. Ramirez, W. Bao and S. -W. Cheong: Phys. Rev. Lett. **75** (1995) 3336.
[21] M. Yamanaka and N. Nagaosa: J. Phys. Soc. Jpn. **65** (1996) 3088.
[22] G. Tatara and H. Fukuyama: Phys. Rev. Lett. **78** (1997) 3773.
[23] P. M. Levy and S. Zhang, Phys. Rev. Lett. **79** (1997) 5110.
[24] A. Brataas, G. Tatara and G. Bauer, Phil. Mag. B **78** (1998) 545.
[25] A. Brataas, G. Tatara and G. Bauer, submitted to Phys. Rev. **B**.
[26] J. B. A. N. van Hoof, K. M. Schep, A. Brataas, G. Bauer and P. J. Kelly: Phys. Rev. **B59** (1999) 138.
[27] G. Tatara Y.-W. Zhao, M. Muñoz and N. García: preprint.
[28] N. Garcia, M. Munoz and Y. W. Zhao, to appear in Phys. Rev. Lett. (1999).
[29] T. Ono, H. Miyajima, K. Shigeto and T. Shinjo: Appl. Phys. Lett. **72** (1998) 1116.
[30] K. Mibu, T. Nagahama, T. Shinjo and T. Ono: Phys. Rev. **B58** (1998) 6442.
[31] S. Yamada, T. Kikutani, N. Aoki, H. Hori and G. Tatara: Phys. Rev. Lett. **81** (1998) 5422.
[32] G. Bergmann, Phys. Reports **107** (1984) 1.
[33] P. A. Lee and T. V. Ramakrishnan, Rev. Mod. Phys. **57** (1985) 287.
[34] T. L. Meisenheimer and N. Giordano, Phys. Rev. **B39** (1989) 9929.
[35] S. Feng, P. A. Lee and A. D. Stone, Phys. Rev. Lett. **56** (1986) 1960.
[36] P. A. E. Jonkers, S. J. Pickering, H. De Raedt and G. Tatara, submitted to Phys. Rev. **B**, preprint cond-mat/9902340.
[37] Y. L.-Geller, I. L. Aleiner and P. M. Goldbart: Phys. Rev. Lett. **81** (1998) 3215.
[38] D. Loss, H. Schoeller and P. M. Goldbart: Phys. Rev. **B** (1999) to appear.
[39] G. Tatara and H. Fukuyama: preprint cond-mat/9902256. 3773.
[40] M. Giroud, H. Courtois, K. hasselbach, D. Mailly and B. Pannetier: Phys. Rev. **B58** (1998) R11872.
[41] K. Ono, H. Shimada and Y. Ootuka: J. Phys. Soc. Jpn. **66** (1997) 1261.
[42] B. Golding, N. M. Zimmerman and S. N. Coppersmith: Phys. Rev. Lett. **68** (1992) 998.
[43] K. A. Meyer and M. B. Weissman: Phys. Rev. **B51** (1995) 8221.
[44] C. Strunk, M. Henny, C. Schoenenberger, G. Neuttiens and C. van Haesendonck: Phys. Rev. Lett. **81** (1998) 2982.
[45] F. Coppinger , J. Genoe, D. K. Maude, Ulf Gennser, J. C. Portal, K. E. Singer, P. Rutter, T. Taskin, A. R. Peaker and A. C. Wright: Phys. Rev. Lett. **75** (1994) 3513.
[46] *Quantum Tunneling of Magnetization*, L. Gunther and B. Barbara (eds.) (Proc. NATO workshop, Chichilianne, France, June 1994), Kluwer Publishing (1995).
[47] E. M. Chudnovsky and L. Gunther: Phys. Rev. Lett. **60** (1988) 661.
[48] A. O. Caldeira and A. J. Leggett: Phys. Rev. Lett. **46** (1981) 211; A. O. Caldeira and A. J. Leggett: Ann. Phys. **149** (1983) 374.
[49] L. Balcells, J. L. Tholence, S. Linderoth, B. Barbara and J. Tejada: Z. Phys. **B89** (1992) 209.
[50] B. Barbara, L. C. Sampaio, J. E. Wegrowe, B. A. Ratnam, A. Marchand, C. Paulsen, M. A. Novak, J. L. Tholence, M. Uehara and D. Fruchart: J. Appl. Phys. **73** (1993) 6703.
[51] C. Paulsen, J. -G. Park, B. Barbara, R. Sessoli and A. Caneschi: J. Magn. Mater. **140-144** (1995) 379.
[52] J. R. Friedman, M. P. Sarachik, J. Tejada and R. Ziolo: Phys. Rev. Lett. **76** (1996) 3830; J. M. Hernandez, X. X. Zhang, F. Luis, J. Tejada, J. R. Friedman, M. P. Sarachik and R. Ziolo: Phys. Rev. **B55** (1997) 5858.
[53] D. D. Awaschalom, J. F. Smyth, G. Grinstein, D. P. DiVincenzo and D. Loss: Phys. Rev. Lett. **71** (1993) 4276.
[54] A. Garg: Phys. Rev. Lett. **71** (1993) 4249.

[55] S. Gider, D. D. Awashalom, T. Douglas, S. Mann and M. Chaparala: Sicence **268** (1995) 77.
[56] J. Tejada, X. X. Zhang, E. del Barco, J. M. Hernndez and E. M. Chudnovsky: Phys. Rev. Lett. **79** (1997) 1754.
[57] M. Lederman, S. Schultz and M. Ozaki: Phys. Rev. Lett. **73** (1994) 1986.
[58] W. Werndorfer et al.: J. Magn. Magn. Mater. **145**, 33 (1995).
[59] D. D. Awaschalom and D. P. DiVincenzo: Physics Today **48** (1995) 43 .
[60] W. Werndorfer, E. B. Orozco, K. Hasselbach, A. Benoit, B. Barbara, N. Demoncy, A. Loiseau, H. Pascard and D. Mailly, Phys. Rev. Lett. **78** (1997) 1791.
[61] P. C. E. Stamp: Phys. Rev. Lett. **66** (1991) 2802.
[62] G. Tatara and H. Fukuyama: Phys. Rev. Lett. **72** (1994) 772; J. Phys. Soc. Jpn. **63**(1994) 2538 .
[63] W. Werndorfer, B. Doudin, D. Mailly, K. Hasselbach, A. Benoit, J. Meier, J. -Ph. Ansermet and B. Barbara: Phys. Rev. Lett. **77** (1996) 1873.
[64] H-B. Braun and D. Loss: Phys. Rev. **B53** (1996) 3237.
[65] S. Takagi and G. Tatara: Phys. Rev. **B54** (1996) 9920.
[66] H. Mori: Prog. Theor. Phys. **33**(1965) 423 ; **34** (1965) 399; W. Götze and P. Wölfle: Phys. Rev. **B6** (1972) 1226.
[67] B. L. Altshuler, A. G. Aronov and D. E. Khmelnitsky: J. Phys. C: Solid State Phys. **15** (1982) 7367.
[68] P. A. Lee and A. D. Stone: Phys. Rev. Lett. **55** (1985) 1622; P. A. Lee, A. D. Stone and H. Fukuyama: Phys. Rev. **B35** (1987) 1039.

FIG. 1. A configuration of a domain wall in a mesoscopic wire.

FIG. 2. The contributions to the Boltzmann conductivity which are the second order with respect to the interaction with the domain wall, denoted by wavy lines. Solid lines indicate the electron Green functions and the current vertex (expressed by crosses) with wavy line represents δJ.

FIG. 3. Shift of the electron density due to the second order interaction with the domain wall.

FIG. 4. (a): Particle-particle ladder (Cooperon) in the absence of domain wall. Dotted line denotes the impurity scattering. This process is singular at $q \sim 0$ if $\omega_n \cdot \omega_{n'} < 0$. (b): Particle-hole ladder (Diffuson) process. This process is also singular at $\mathbf{q} \sim \mathbf{k} + \mathbf{q}'$ but does not contribute to the quantum correction to the conductivity.

FIG. 5. Quantum correction to the conductivity expressed in terms of Cooperon. Cooperon is defined by Fig. 4(a), but it is twisted here (maximally crossed diagram).

FIG. 6. Effect of domain wall on the Cooperon to the second order. Hatched square denotes the particle-particle ladder (Cooperon). (a): Self-energy type. This is the dominant process. Process (b) contains only one Cooperon and thus gives smaller contribution compared to (a). Process (c) and the vertex correction type (d)(e) include Cooperon(s) with different spins, and thus are suppressed in ferromagnets ($\Delta\tau/\hbar \gg 1$).

FIG. 7. Higher order orrection by the wall to the Cooperon which represents a dephasing time by the wall.

FIG. 8. Contributions to the conductance change due to the motion of the wall over a distance of r at the lowest (fourth) order of domain wall interaction. Processes with four Cooperons are shown here. The domain wall is at $z = r$ and $z = 0$ in outer and inner loop, respectively. n and $n + \ell$ denotes the Matsubara frequencies ω_n and $\omega_{n+\ell}$, respectively. (a) and (a') are different in the Matsubara frequencies of the internal loop. Current vertices are denoted by crosses.

FIG. 9. Particle-particle ladder which includes the motion of the domain wall. One of the electron line here interacts with the wall at $z = r$ and the other with the wall at $z = 0$.

FIG. 10. Contributions to the conductance change containing five Cooperons. Although they contains more Cooperons their contributions are the same order as four Cooperons processes. Diagrams (i)(ii)(iii) correspond to three different contributions which is obtained by cyclic replacement of $\delta\Gamma$'s and Γ. In processes (b)-(d) only one of such contribution is shown.

FIG. 11. Contributions to the conductance change containing six Cooperons.

FIG. 12. The contour C_0 of integration in complex z-plane appeared in the summation over the Matsubara frequencies. Because of the function $f(z)$, there are poles on the imaginary axis at $z = (2n-1)\pi i/\beta$ where $n = 0, \pm 1, \pm 2 \cdots$. C_1 is a deformed contour parallel to the real axis.

FIG. 13. The contour of integration C_2 in complex ϵ-plane. There is a cut on the real axis from $\epsilon = -\epsilon_F$ to $+\infty$, because of the behavior of the density of states, $N(\epsilon) \propto (\epsilon + \epsilon_F)^{1/2}$ in three-dimensions.

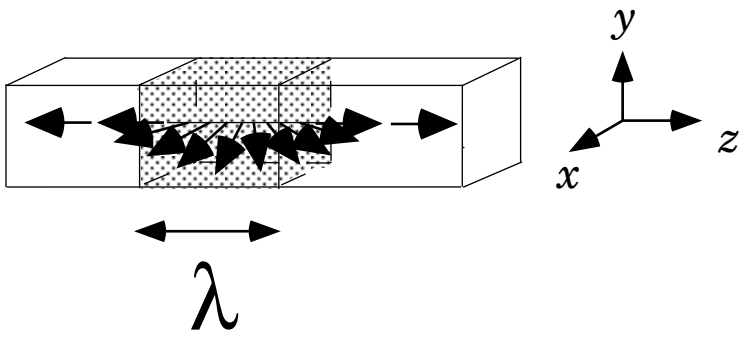

G. Tatara Fig. 1

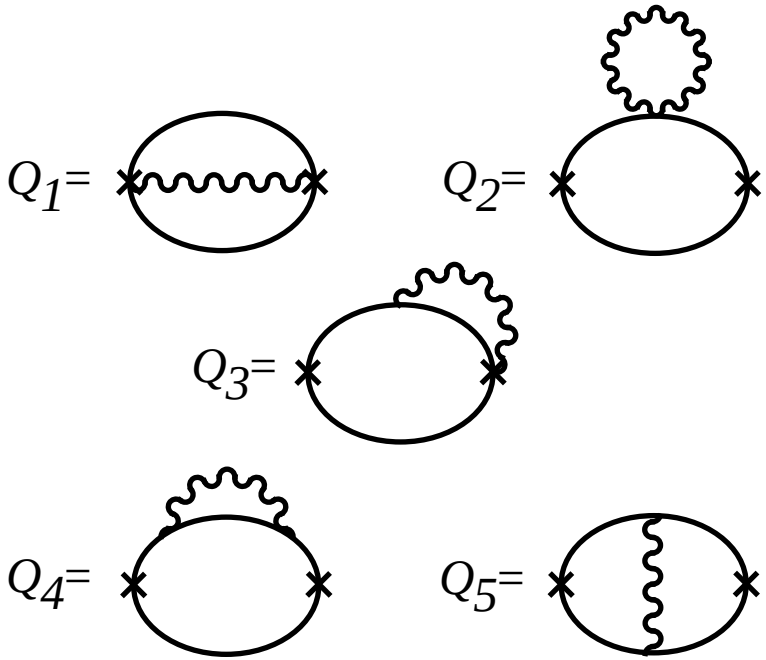

G. Tatara Fig.2

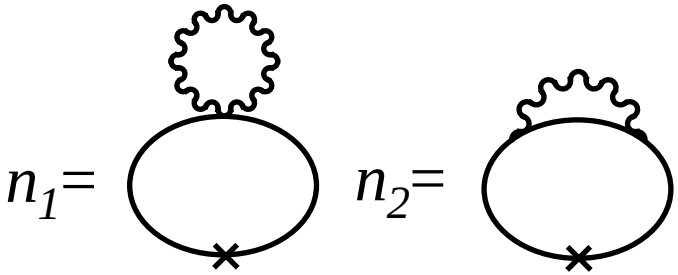

G. Tatara Fig. 3

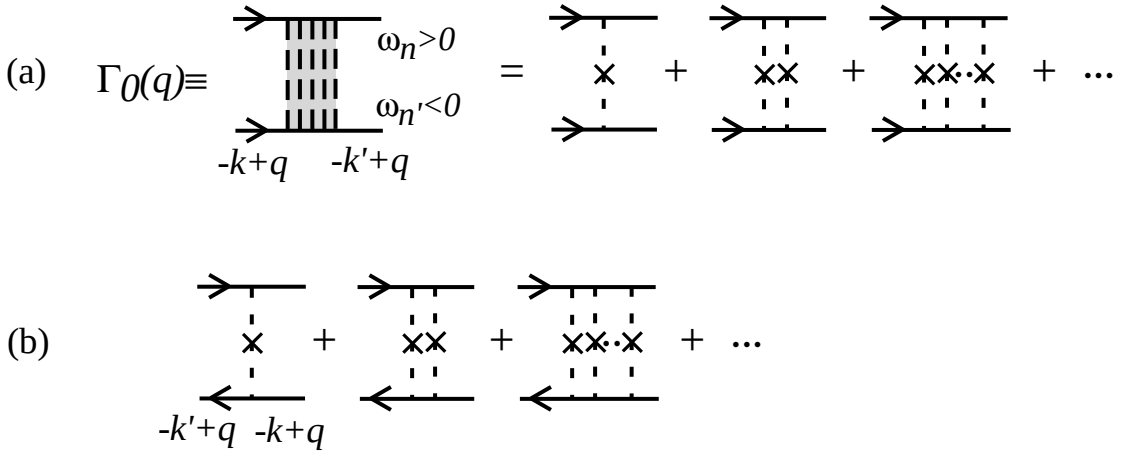

G. Tatara Fig. 4

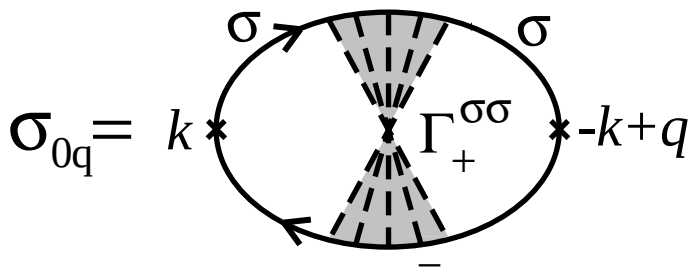

G. Tatara Fig. 5

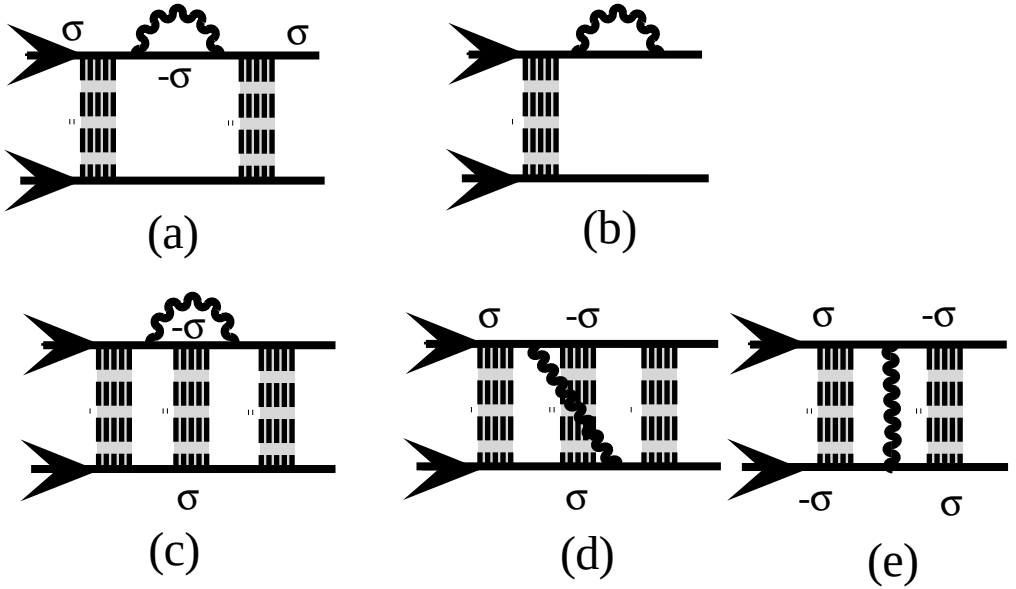

G. Tatara Fig. 6

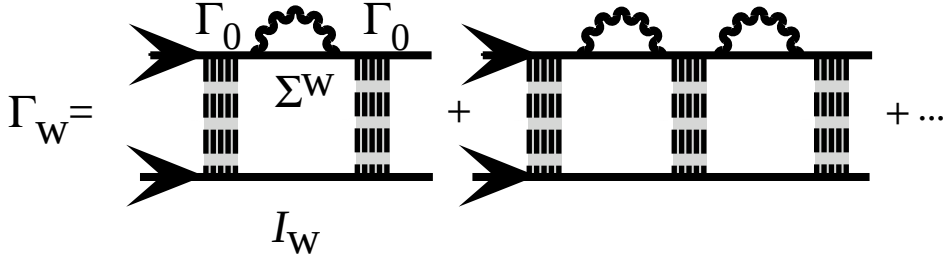

G. Tatara Fig.7

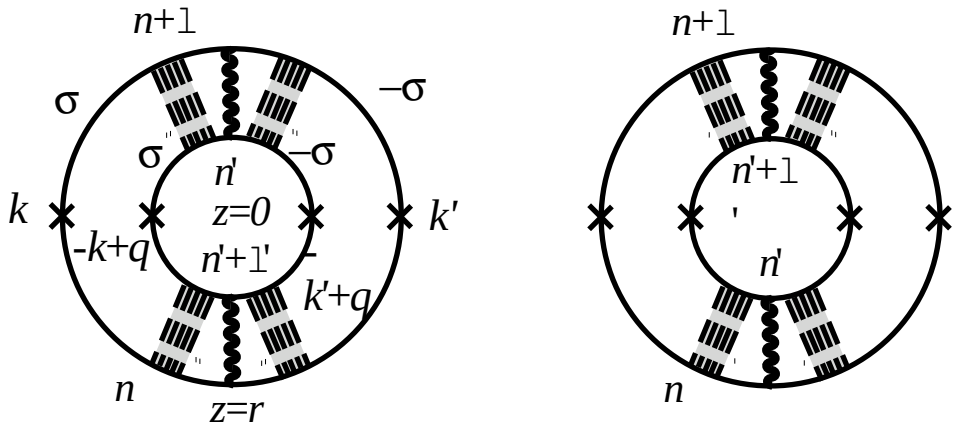

G. Tatara Fig. 8

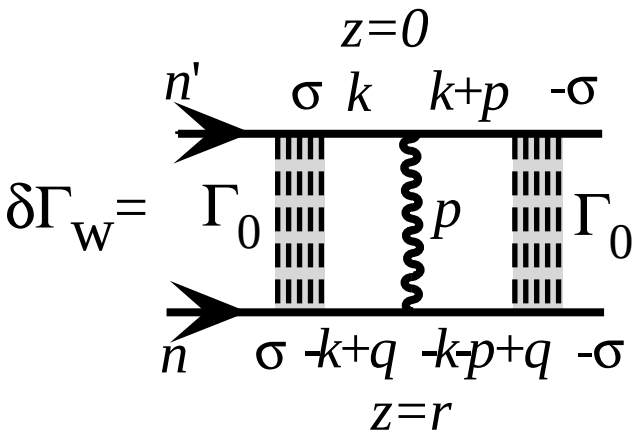

G. Tatara Fig. 9

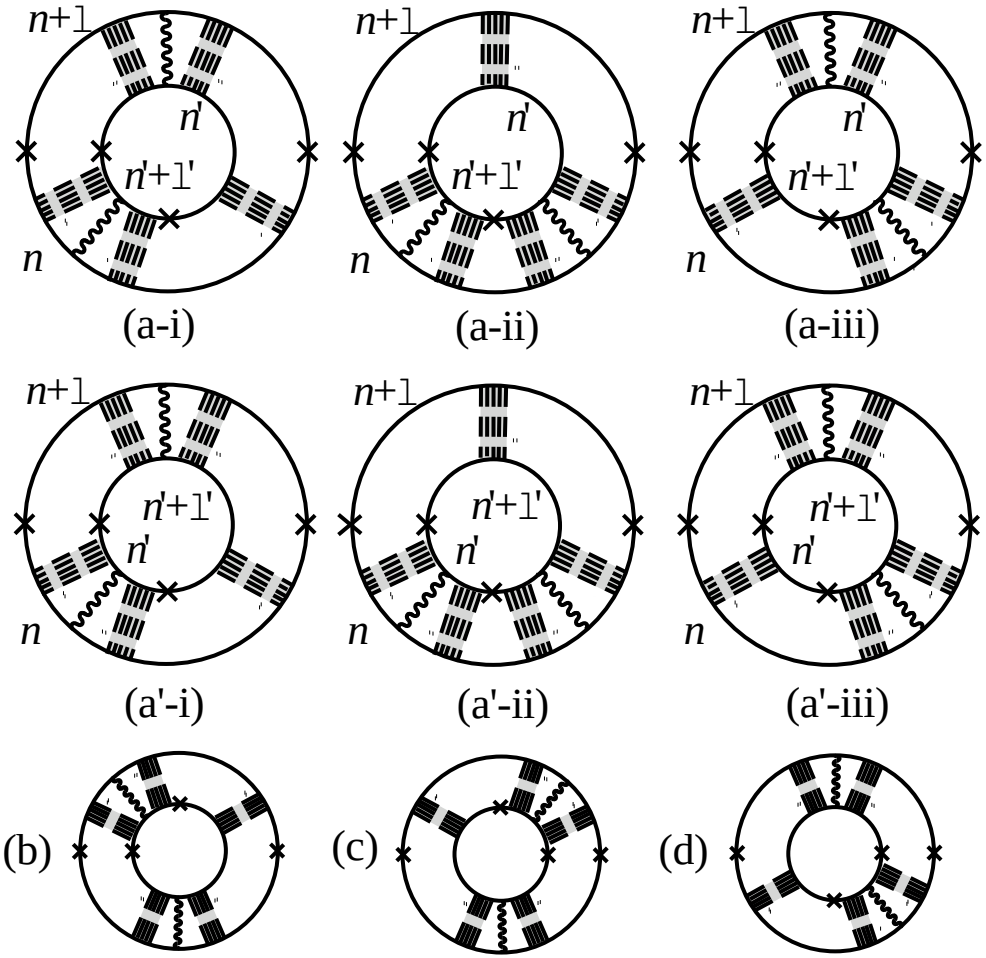

G.Tatara Fig. 10

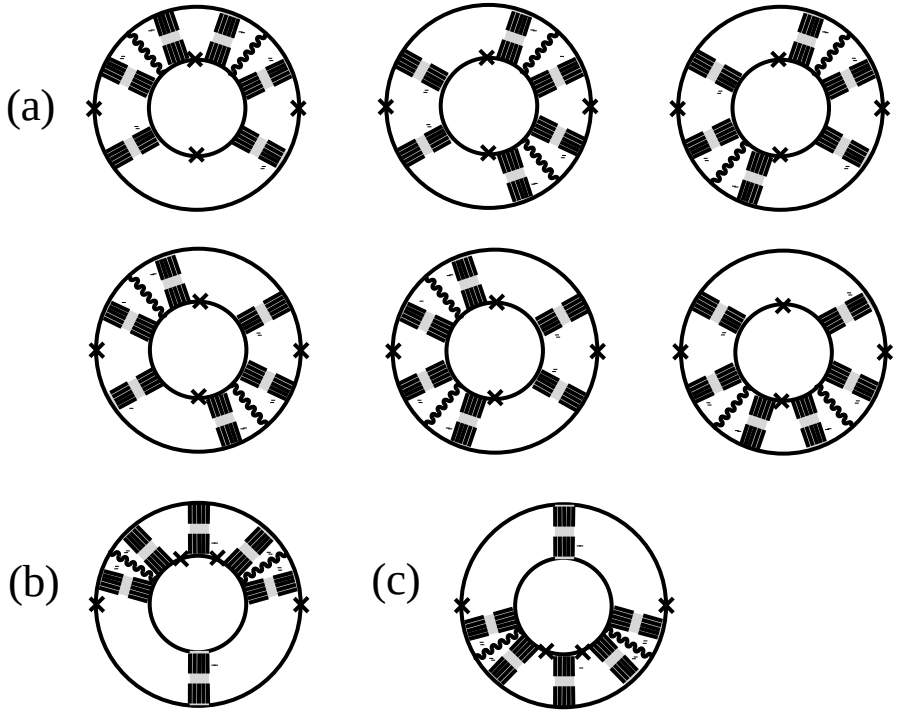

G. Tatara Fig. 11

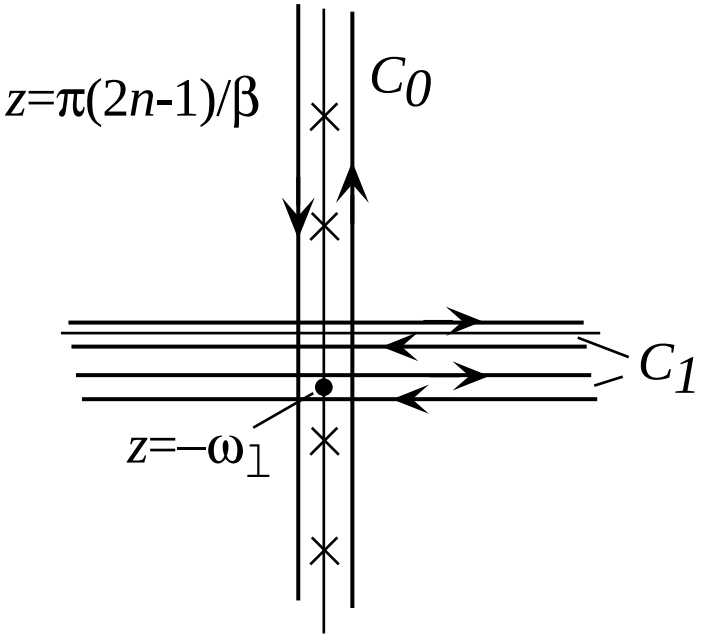

G. Tatara Fig. 12

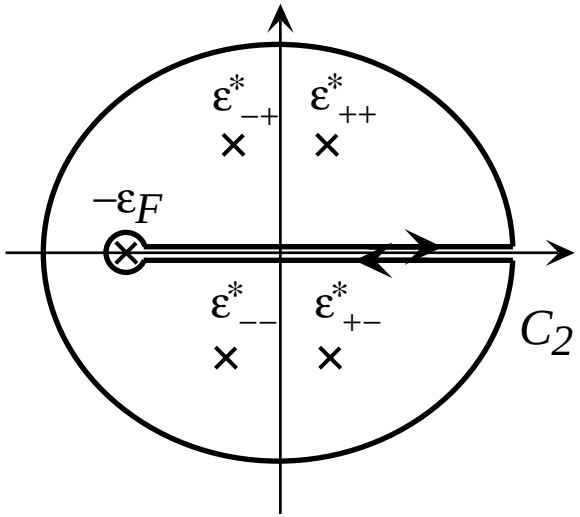

G. Tatara Fig. 13